Dilepton production at finite temperature: Perturbative treatment at order α_s

R. Baier
Fakultät für Physik, Universität Bielefeld, D-4800 Bielefeld, Federal Republic of Germany

B. Pire
Centre de Physique Théorique, École Polytechnique, F-91128 Palaiseau Cedex, France

D. Schiff
Laboratoire de Physique Théorique et Hautes Energies, Université Paris-Sud, Bâtiment 211, F-91405 Orsay, France
(Received 3 August 1988)

In the framework of finite-temperature perturbative QCD we examine the first-order corrections to the rate of lepton pairs produced in a thermalized quark-gluon plasma. The dilepton rate is calculated using the real-time formalism in two different ways by (i) applying the Feynman amplitude approach and by (ii) analyzing the relationship to the discontinuity of the two-loop photon self-energy at finite temperature. We mainly study the infrared and mass singular behavior and we show that up to order α_s the rate is free of these divergences in the limit of vanishing gluon and quark masses.

I. INTRODUCTION

The existence of a new phase of matter, the quark-gluon-plasma phase, at high temperature T or/and density, is one of the most remarkable predictions of QCD (Ref. 1). A number of experimental signals for the observation of the formation of this deconfined phase in ultrarelativistic heavy-ion collisions have been proposed and are extensively discussed.[2] Among these signals, lepton pairs produced through a thermal Drell-Yan mechanism have attracted much attention. A number of questions concerning the details of the production mechanism have already been treated.[3,4] In this paper we focus on the validity of the perturbative expansion in the QCD coupling up to $O(\alpha_s)$ for the dilepton production rate assuming the existence of a thermalized quark-gluon plasma.

The real-time formalism[5] of relativistic quantum field theory at finite temperature is used throughout this paper. In Sec. II we briefly present this formalism. We show the main steps leading to the perturbative expansion in terms of Feynman diagrams of the thermal vacuum expectation value of the product of electromagnetic currents, which is the object of interest. In Sec. III we study the $O(\alpha_s)$ corrections to the dilepton rate, using this approach which follows rather closely Ref. 6. We mainly focus on the infrared (IR) and mass singular behavior of the dilepton rate. The motivation is the following.

(i) The IR region presents new features at $T\neq 0$, since the presence of the Bose-Einstein factor, which behaves as $1/k$ for small gluon energies k, worsens the infrared behavior of $O(\alpha_s)$ contributions compared to the $T=0$ case.

(ii) The mass singularities attached to the emission or absorption of a collinear gluon by a massless quark may also not cancel. The Kinoshita-Lee-Nauenberg (KLN) theorem[7] does not apply at finite temperature. On the other hand, the finite-T dilepton production is altogether different from the $T=0$ Drell-Yan process at high energies. There mass singular terms are absorbed into parton distribution functions according to the prescriptions of the factorization theorem,[8] whereas at $T\neq 0$ summation over all phase space is performed. Although at finite-temperature fermion masses get temperature-dependent contributions, which would shield these mass singularities, the question of the presence of large terms proportional to $\ln[1/\alpha_s(T)]$ (Ref. 9) in the rate at $O(\alpha_s)$ is crucial.

(iii) From the phenomenological point of view it is an important question to check the validity of the Born approximation for dilepton production in order to be able to present safe predictions for this signal. Indeed, the Drell-Yan process at zero temperature is considered as a good test of perturbative QCD, because higher-order corrections to the cross section are well under control.

In the intermediate steps of our calculation we regularize these singularities by giving masses to quarks and gluons and we show that finally the dilepton rate, at least at $O(\alpha_s)$, is free of divergences in the limit of vanishing masses.[10] Our calculation is performed for the lepton pair at rest with respect to the plasma. We also assume a vanishing chemical potential. This helps to simplify the algebraic expressions and the integrals without altering the singularity structure.

Section IV is devoted to an alternative approach for calculating lepton-pair production at finite temperature. By analogy to the QCD analysis of the total hadronic e^+e^- cross section at zero temperature, we relate the dilepton rate to the imaginary part of the electromagnetic vacuum-polarization tensor, which is then directly evaluated at the two-loop level. This procedure extends the discussions by Weldon[11] and by Kobes and Semenoff[12,13] on the issue of rates derived from discontinuities of self-

energy functions at finite temperature. This elegant approach reproduces the results presented in Sec. III. It allows showing in general the absence of ill-defined δ^2 (or pinch) singularities in the rate, calculated with real-time methods;[13] whereas in Sec. III we have to rely on the regularization procedure. The final section, Sec. V, contains our conclusions.

II. THEORETICAL FRAMEWORK

Field theory at finite temperature has been studied for a long time using different techniques.[14] In order to calculate production rates one should apply the real-time formalism which, contrary to the Matsubara imaginary-time technique,[15] allows to directly calculate transition amplitudes beyond the leading order. A recent formulation of the real-time finite-temperature field theory has been developed by Umezawa *et al.*[5] as thermo field dynamics. This formalism allows us to derive a perturbative expansion for the dilepton production rate in the plasma at finite temperature $T=1/\beta$, in a similar way as at zero temperature.

The main features of this approach may be briefly summed up before we discuss the detailed calculation of the rate.

Physical states are constructed from a temperature-dependent vacuum $|0(\beta)\rangle$. The thermal average of any operator A is equal to its temperature-dependent vacuum expectation value

$$\langle A \rangle_\beta = \langle 0(\beta) | A | 0(\beta) \rangle . \tag{2.1}$$

Doubling of degrees of freedom of all fields is required. This is achieved through a "tilde" operation: to each zero-temperature field $\Phi(x)$ a doublet of fields $(\Phi(x), \tilde{\Phi}^\dagger(x))$ is attached, the dynamics of which is controlled by a thermal Lagrangian

$$\mathcal{L} = \mathcal{L}(\Phi) - \tilde{\mathcal{L}}(\Phi) = \mathcal{L}(\Phi) - \mathcal{L}^*(\tilde{\Phi}) . \tag{2.2}$$

The thermal doublet of fields is denoted by $(\Phi_1(x), \Phi_2(x))$ in the following and one speaks of type-1 and type-2 fields, respectively.

The temperature-dependent vacuum state is annihilated by physical annihilation operators: $a(\beta,k)$ and $\tilde{a}(\beta,k)$ for bosons and $b_\pm(\beta,p)$ and $\tilde{b}_\pm(\beta,p)$ for fermions, respectively, which are obtained through a Bogoliubov transformation[5] from the usual annihilation operators $a(k)$ $[b_\pm(p)]$ and their tilde partners. The Bogoliubov parameter is related to the temperature once one fixes the thermal expectation value of number operators to be a Bose-Einstein $[n_B(k)]$ or Fermi-Dirac $[n_F(p)]$ distribution. For the boson case the transformation reads

$$\begin{bmatrix} a(\beta,k) \\ \tilde{a}^\dagger(\beta,k) \end{bmatrix} = \begin{bmatrix} \cosh\theta_k & -\sinh\theta_k \\ -\sinh\theta_k & \cosh\theta_k \end{bmatrix} \begin{bmatrix} a(k) \\ \tilde{a}^\dagger(k) \end{bmatrix} , \tag{2.3}$$

where

$$\sinh^2\theta_k = n_B(k) = \frac{1}{e^{\beta|k_0|}-1} . \tag{2.4}$$

In the case of fermions the analogous expressions are

$$\begin{bmatrix} b_\pm(\beta,p) \\ \tilde{b}^\dagger_\pm(\beta,p) \end{bmatrix} = \begin{bmatrix} \cos\phi_p & -\sin\phi_p \\ \sin\phi_p & \cos\phi_p \end{bmatrix} \begin{bmatrix} b_\pm(p) \\ \tilde{b}^\dagger_\pm(p) \end{bmatrix} , \tag{2.5}$$

where

$$\sin^2\phi_p = n_F(p) = \frac{1}{e^{\beta|p_0|}+1} . \tag{2.6}$$

From the usual $T=0$ expansion in terms of creation and annihilation operators of the free field, e.g., for fermions,

$$\psi_0(x) = \int \frac{d^4p}{(2\pi)^3}\theta(p_0)\delta(p^2-m^2) \times [b_+(p)u(p)e^{-ip\cdot x} + b_-^\dagger(p)v(p)e^{ip\cdot x}] , \tag{2.7}$$

one obtains with the transformation Eq. (2.5) then the corresponding expansion in terms of thermal operators (similarly for the tilde partners).

These properties lead to 2×2 matrix propagators, for which one may separate a temperature-independent and a temperature-dependent part. With the notation of Refs. 12 and 16 the free vector-boson propagator (in the Feynman gauge) is

$$D_{ab}^{\mu\nu}(k) = -g^{\mu\nu}D_{ab}(k) \tag{2.8}$$

and

$$iD_{ab}(k) = U(\beta,k) \begin{bmatrix} D(k) & 0 \\ 0 & D^*(k) \end{bmatrix} U(\beta,k) , \tag{2.9}$$

with the matrix U given by

$$U(\beta,k) = \begin{bmatrix} \cosh\theta_k & \sinh\theta_k \\ \sinh\theta_k & \cosh\theta_k \end{bmatrix} \tag{2.10}$$

and

$$D(k) = \frac{i}{k^2-\lambda^2+i\varepsilon} \tag{2.11}$$

(assuming a mass λ for later regularization purposes). In a more explicit form we have

$$iD_{ab}(k) = \begin{bmatrix} D(k) & 0 \\ 0 & D^*(k) \end{bmatrix} + 2\pi\delta(k^2-\lambda^2) \begin{bmatrix} \sinh^2\theta_k & \frac{1}{2}\sinh 2\theta_k \\ \frac{1}{2}\sinh 2\theta_k & \sinh^2\theta_k \end{bmatrix} . \tag{2.12}$$

Separating off the Dirac operator $(\not{p}+m)$ the propagator of a free fermion with mass m is represented by

$$S_{ab}(p)=(\not{p}+m)\tilde{S}_{ab}(p)\ , \tag{2.13}$$

$$S(p)=(\not{p}+m)\tilde{S}(p)=\frac{i(\not{p}+m)}{p^2-m^2+i\varepsilon}\ , \tag{2.14}$$

and

$$i\tilde{S}_{ab}(p)=V(\beta,p)\begin{bmatrix}\tilde{S}(p) & 0\\ 0 & \tilde{S}^*(p)\end{bmatrix}V(\beta,p)\ , \tag{2.15}$$

with the transformation matrix

$$V(\beta,p)=\begin{bmatrix}\cos\phi_p & -\epsilon(p_0)\sin\phi_p\\ \epsilon(p_0)\sin\phi_p & \cos\phi_p\end{bmatrix}\ . \tag{2.16}$$

More explicitly we write

$$i\tilde{S}_{ab}(p)=\begin{bmatrix}\tilde{S}(p) & 0\\ 0 & \tilde{S}^*(p)\end{bmatrix}-2\pi\delta(p^2-m^2)\begin{bmatrix}\sin^2\phi_p & \frac{1}{2}\epsilon(p_0)\sin 2\phi_p\\ -\frac{1}{2}\epsilon(p_0)\sin 2\phi_p & \sin^2\phi_p\end{bmatrix}\ . \tag{2.17}$$

In Sec. IV we also need the full fermion propagator, which is assumed to satisfy the Schwinger-Dyson equation[12]

$$i\mathcal{S}_{ab}=iS_{ab}+\sum_{c,d=1,2}iS_{ac}(-i\Sigma_{cd})i\mathcal{S}_{db}\ , \tag{2.18}$$

which may be put into the matrix form

$$i\mathcal{S}_{ab}(p)=V(\beta,p)\begin{bmatrix}\mathcal{S}(p) & 0\\ 0 & \mathcal{S}^*(p)\end{bmatrix}V(\beta,p)\ , \tag{2.19}$$

with

$$\mathcal{S}(p)=\frac{i}{\not{p}-m-\Sigma(p)+i\varepsilon}\ . \tag{2.20}$$

A complex self-energy function $\Sigma(p)$ is introduced, which can be expressed in terms of the elements of the matrix Σ_{ab} (Ref. 12).

There are two types of vertices, types 1 and 2, distinguished by a relative minus sign. Physical external fields are only of type 1.

Within this framework we calculate the production rate of lepton pairs of momentum Q^μ in a plasma of quarks and gluons in equilibrium at temperature T. First we note that the differential rate per unit space-time volume,[4]

$$\frac{d(R/V)}{d^4Q}=-\frac{\alpha^2\sum_q e_q^2}{12\pi^3Q^2}\langle W_\mu^\mu(Q)\rangle\ , \tag{2.21}$$

is expressed in terms of the Fourier transform of the thermal expectation value of the electromagnetic current-current correlation function

$$\langle W^{\mu\nu}(Q)\rangle=\int d^4x\, e^{-iQ\cdot x}\langle 0(\beta)\mid J^\mu(x)J^\nu(0)\mid 0(\beta)\rangle\ . \tag{2.22}$$

In Eq. (2.21) we sum over the different quark flavors with charge e_q, and assume that the mass of the lepton pair is large compared to the masses of the individual leptons.

The main object of interest is therefore the tensor of Eq. (2.22). Since only its trace is required in Eq. (2.21) we introduce the shorthand notation

$$R\equiv-\langle W_\mu^\mu\rangle\ . \tag{2.23}$$

Because we are not interested in the plasma history we call this quantity R "the rate."

In order to evaluate R one has to insert a complete set of thermal states constructed by successive applications of creation operators $b_\pm^\dagger(\beta,p)$, $\tilde{b}_\pm^\dagger(\beta,p)$, $a^\dagger(\beta,k)$, $\tilde{a}^\dagger(\beta,k)$ on the thermal vacuum $\mid 0(\beta)\rangle$. A basic example for describing the process $q\bar{q}\to\gamma^*$ is the "Drell-Yan state" defined by

$$\mid\psi_{\rm DY}(p_1,p_2)\rangle=\tilde{b}_+^\dagger(\beta,p_1)\tilde{b}_-^\dagger(\beta,p_2)\mid 0(\beta)\rangle\ . \tag{2.24}$$

Let us therefore calculate the matrix element

$$\langle 0(\beta)\mid J^\mu(x)\mid\psi_{\rm DY}(p_1,p_2)\rangle\ , \tag{2.25}$$

with the electromagnetic current in terms of quark fields (color indices are suppressed),

$$J^\mu(x)=:\bar{\psi}(x)\gamma^\mu\psi(x):\ . \tag{2.26}$$

The generalized reduction formula[5] gives for any Heisenberg operator an expansion in terms of normal products of free fields. As a first step we single out products of two free fields and write

$$J^\mu(x)=\int d^4x_1d^4x_2:\bar{\psi}_0(x_1)\lambda(\vec{\partial}_{x_1})\langle 0(\beta)\mid T[J^\mu(x)\psi(x_1)\bar{\psi}(x_2)]\mid 0(\beta)\rangle\lambda(-\overleftarrow{\partial}_{x_2})\psi_0(x_2):+\cdots\ , \tag{2.27}$$

where $\lambda(\vec{\partial}_x)$ is defined as the inverse fermion propagator:

$$\lambda(\vec{\partial}_x)S_{ab}(x-y)=i\delta^4(x-y)\delta_{ab}\ . \tag{2.28}$$

As for zero-temperature perturbation theory, fields appearing in the time-ordered product are expressed in terms of free asymptotic fields, those in thermal equilibrium, with the help of a generalized evolution operator $U(t_1,t_2)$, which is constructed from the thermal interaction Hamiltonian operator $\hat{H}_I=H_I-\tilde{H}_I$. The thermal vacuum $|0(\beta)\rangle$ is an eigenstate of this Hamiltonian. This allows us to write the vacuum expectation value appearing in Eq. (2.27) as a perturbative series of finite-temperature expectation values of time-ordered products of free fields. The generalized Wick's theorem[17] then allows expressing this quantity as a product of contractions and, hence, allows us to express the matrix element $\langle 0(\beta)|J^\mu(x)|\psi_{\rm DY}(p_1,p_2)\rangle$ in terms of Feynman diagrams. At lowest order one derives the simple expression for the current operator,

$$J^\mu(x)=\int d^4x_1 d^4x_2 :\bar{\psi}_0(x_1)\lambda(\vec{\partial}_{x_1})\langle 0(\beta)|T[:\bar{\psi}_0(x)\gamma^\mu\psi_0(x):\psi_0(x_1)\bar{\psi}_0(x_2)]|0(\beta)\rangle\lambda(-\overleftarrow{\partial}_{x_2})\psi_0(x_2):+\cdots , \quad (2.29)$$

which sandwiched between $\langle 0(\beta)|$ and the "Drell-Yan state" leads to

$$\langle 0(\beta)|J^\mu(x)|\psi_{\rm DY}(p_1,p_2)\rangle = \sin\phi_{p_1}\sin\phi_{p_2}e^{i(p_1+p_2)\cdot x}\bar{v}(p_2)\gamma^\mu u(p_1) . \quad (2.30)$$

From this expression and integrating on p_1,p_2 with the usual two-particle phase space we find that R, Eq. (2.23), is given, to lowest order for a timelike photon, by

$$R^{\rm Born}=N_C\frac{v}{2\pi}(Q^2+2m^2)n_F^2(Q/2) , \quad (2.31)$$

where $v=(1-4m^2/Q^2)^{1/2}$ and N_C is the number of colors. Other intermediate states lead to kinematically forbidden processes (e.g., $q\to q\gamma^*$) at this order. For simplicity we have assumed the photon to be at rest in the plasma rest frame, $Q^\mu=(Q,0)$. Equation (2.31) is the expected rate: the $T=0$ Drell-Yan Born approximation multiplied by Fermi-Dirac statistical weights.[4]

The above-described procedure allows us to derive, in principle, the Feynman rules for the higher-order contributions to the thermal vacuum expectation value $\langle W^{\mu\nu}(Q)\rangle$, and thus to R. At next-to-leading order the QCD perturbative expansion of the evolution operator together with the insertion of intermediate states including gluons and/or additional quarks and antiquarks leads to the whole series of real (Figs. 2 and 3) and virtual (Figs. 4 and 5) diagrams. The distinctive features of this finite-temperature expansion are the appearance of the 2×2 matrix structure of the propagators [Eqs. (2.12) and (2.17)], due to the tilde fields in $\hat{H}$ and thus in the generalized evolution operator, and of the statistical weights attached to the external particles. With these rules in mind we are now in the position to evaluate the Feynman amplitudes relevant for the dilepton rate up to $O(\alpha_s)$.

III. LEPTON-PAIR PRODUCTION—THE AMPLITUDE APPROACH

The above-described framework allows us to calculate the whole series of perturbative contributions to the lepton pair production rate. The Born contribution (Fig. 1) is given by

$$R^{\rm Born}=\int n_F(E_1)n_F(E_2)M^\mu M_\mu^* d[P] , \quad (3.1)$$

where P is the two-particle phase space and M^μ is the Born amplitude. For the photon at rest this leads to Eq. (2.31) of the previous section. Corrections at $O(\alpha_s)$ involve real and virtual diagrams shown in Figs. 2–5. Each propagator has the structure of Eq. (2.12) for the gluon and of Eq. (2.17) for the quark, respectively. In the following we treat separately its temperature-dependent part, which is represented by a slashed line in Figs. 2–5.

As discussed earlier the contribution of each class of diagrams is given by the Feynman amplitude squared $M^\mu M_\mu^*$ with appropriate statistical factors attached to external legs. We include these factors into the phase-space integrals.

The IR and collinear singularities are regularized by giving masses λ and m to gluons and quarks, respectively. The explicit calculations are performed for the special kinematical configuration, in which the photon is at rest with respect to the heat bath.

A. Real diagrams

In this case, since external fields are of type 1, we only deal with propagators for "1" fields. Moreover, we only have to consider nonslashed propagators as argued in the following.

The contribution associated with the temperature-dependent (slashed) part of the quark propagator involves δ functions: e.g., for the diagram of Fig. 3(a) and its crossed counterpart we find terms proportional to $[\delta(t-m^2)]^2$ or $[\delta(u-m^2)]^2$, typically ill-defined singular terms, and to $\delta(t-m^2)\delta(u-m^2)$, where $t(u)=(p_1-k)^2[(p_2-k)^2]$. Because of the regularization mass λ these terms vanish in the physical region. Thus, in accordance with the regularization procedure, they do not contribute in the limit $\lambda\to0$.

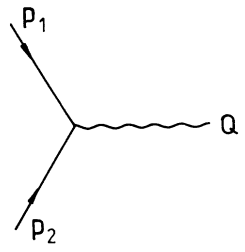

FIG. 1. Born diagram for heavy photon (dilepton) production. The photon is denoted by a wavy line.

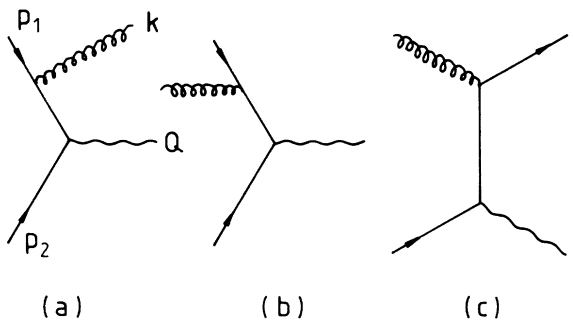

FIG. 2. Feynman diagrams for (a) real emission; (b) real absorption of a gluon (curly line); (c) Compton scattering. The crossed diagrams are not shown.

It is important, however, to discuss in a more general way the cancellation of the ill-defined δ^2 singularities, when calculating rates. This is done in more detail in Sec. IV.

1. Calculation

The phase-space integral for gluon emission [Fig. 2(a)] is written as

$$P_{\rm em}=\frac{1}{4}\frac{1}{(2\pi)^3}\int_\lambda^\infty d\omega\int_{E_{\rm min}}^{E_{\rm max}}dE_1 n_F(E_1)n_F(E_2)\times[1+n_B(\omega)]\,, \tag{3.2}$$

where $\omega,E_1,E_2=Q+\omega-E_1$ are the energies attached to k,p_1,p_2. The bounds of integration are

$$E_{\rm min}^{\rm max}=\frac{Q+\omega}{2}\pm\frac{\kappa}{2}\left[1-\frac{4m^2}{Q(Q+2\omega)+\lambda^2}\right]^{1/2}, \tag{3.3}$$

with $\kappa=(\omega^2-\lambda^2)^{1/2}$.

For gluon absorption [Fig. 2(b)] conservation of energy and momentum implies that $\omega\le\omega_{\rm max}$ with $\omega_{\rm max}=\frac{1}{2}(Q+\lambda^2/Q-4m^2/Q)$. In this case the energy E_1 runs between $\bar{E}_{\rm min}$ and $\bar{E}_{\rm max}$,

$$\bar{E}_{\rm min}^{\rm max}=\frac{Q-\omega}{2}\pm\frac{\kappa}{2}\left[1-\frac{4m^2}{Q(Q-2\omega)+\lambda^2}\right]^{1/2}. \tag{3.4}$$

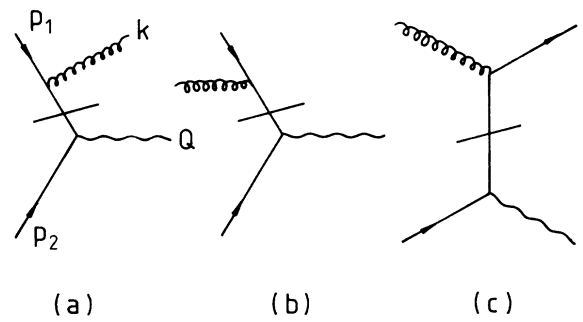

FIG. 3. The same diagrams as in Fig. 2, but with temperature-dependent quark propagators (slashed line).

The phase-space integral is given by

$$P_{\rm abs}=\frac{1}{4}\frac{1}{(2\pi)^3}\int_\lambda^{\omega_{\rm max}}d\omega\int_{\bar{E}_{\rm min}}^{\bar{E}_{\rm max}}dE_1 n_F(E_1)n_F(E_2)n_B(\omega)\,, \tag{3.5}$$

with $E_2=Q-\omega-E_1$.

Finally, in the Compton case [Fig. 2(c)] we find

$$P_{\rm Compton}=\frac{1}{4}\frac{1}{(2\pi)^3}\int_{\omega_m}^\infty d\omega\int_{\bar{E}}^\infty dE_1 n_F(E_1)\times[1-n_F(E_2)]n_B(\omega)\,, \tag{3.6}$$

with

$$\bar{E}=\frac{Q-\omega}{2}+\frac{\kappa}{2}\left[1+\frac{4m^2}{Q(2\omega-Q)-\lambda^2}\right]^{1/2}, \tag{3.7}$$

where $\omega_m=\frac{1}{2}(Q+\lambda^2/Q)$ and $E_2=\omega+E_1-Q$.

Let us write down the rate in the case of emission:

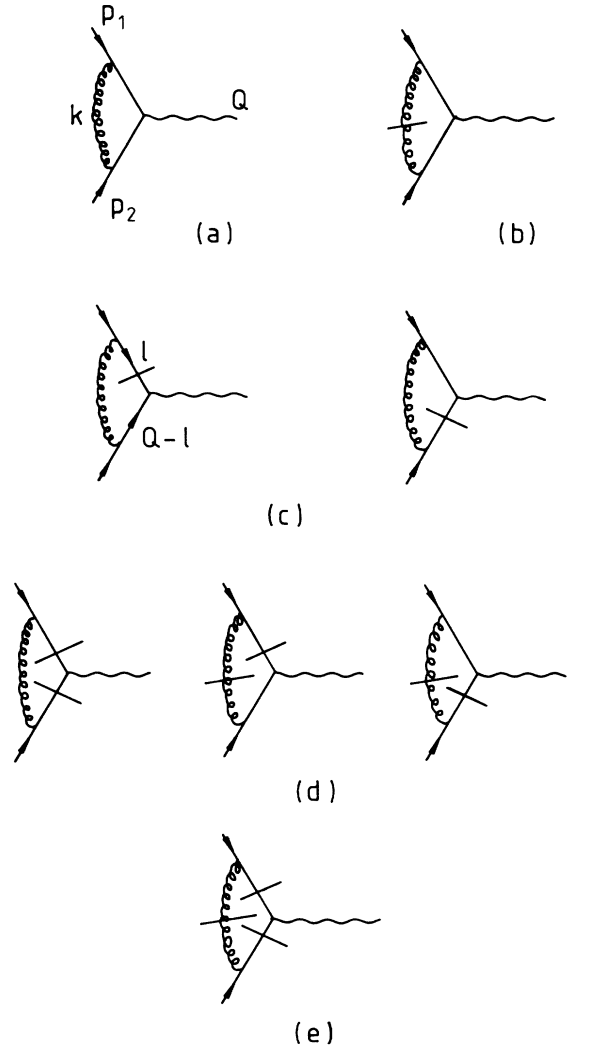

FIG. 4. Feynman diagrams for the vertex corrections. The temperature-dependent propagators are represented by a slashed line.

$$R_{\rm em}=-4\frac{\alpha_s}{\pi^2}N_C C_F\int_\lambda^\infty d\omega[1+n_B(\omega)]\int_{E_{\rm min}}^{E_{\rm max}}dE\, n_F(E)n_F(Q+\omega-E)$$
$$\times\left[\frac{1}{2}+\frac{1}{2Q(E-Q/2)}\left[-Q^2-Q\omega-2m^2-\frac{Q^3}{2\omega}+\frac{2m^4}{Q\omega}\right]\right.$$
$$\left.+\frac{m^2(2m^2+Q^2)}{4Q^2(E-Q/2)^2}+O(\lambda^2)\right], \tag{3.8}$$

with $C_F=\frac{1}{2}(N_C^2-1)/N_C$.

The absorption rate is obtained by substituting $\omega\to-\omega$ in the above integrand and using the corresponding phase space Eq. (3.5).

2. *Isolating mass singularities*

In order to exhibit the mass singularities in Eq. (3.8) we expand the statistical weights $n_F(E)$ and $n_F(Q+\omega-E)$ in the vicinity of the pole $E=Q/2$:

$$n_F(E)=n_F(Q/2)+\tilde{n}_F(E) \tag{3.9}$$

and

$$n_F(Q+\omega-E)=n_F(Q/2+\omega)+\tilde{n}'_F(E)\,, \tag{3.10}$$

where $\tilde{n}_F(E)$ and $\tilde{n}'_F(E)$ behave as $O(E-Q/2)$ so that

$$n_F(E)n_F(Q+\omega-E)=n_F(Q/2)n_F(Q/2+\omega)$$
$$+O(E-Q/2)\,. \tag{3.11}$$

It is easy to see by inspection of Eq. (3.8) that the term behaving as $O(E-Q/2)$ does not lead to any IR or mass singular contributions. Keeping only the singular terms we are then led to the following expression for the emission rate:

$$R^S_{\rm em}=-4\frac{\alpha_s}{\pi^2}N_C C_F\int_\lambda^\infty d\omega[1+n_B(\omega)]n_F(Q/2)$$
$$\times n_F(Q/2+\omega)\mathcal{E}_1\,, \tag{3.12}$$

where $\mathcal{E}_1$ is given by

$$\mathcal{E}_1=-\frac{1}{2}\left[Q+\omega+\frac{1}{2\omega Q^2}(Q^4-4m^4)\right]I_1^S$$
$$+\frac{m^2}{4Q^2}(Q^2+2m^2)I_2^S\,. \tag{3.13}$$

The quantities $I_1^S(\omega)$ and $I_2^S(\omega)$ are the singular parts of the following integrals:

$$I_1(\omega)=\int_{E_{\rm min}}^{E_{\rm max}}\frac{dE}{E-Q/2}$$
$$=\ln\left[\frac{\omega+\kappa\left[1-\dfrac{4m^2}{Q(Q+2\omega)+\lambda^2}\right]^{1/2}}{\omega-\kappa\left[1-\dfrac{4m^2}{Q(Q+2\omega)+\lambda^2}\right]^{1/2}}\right] \tag{3.14}$$

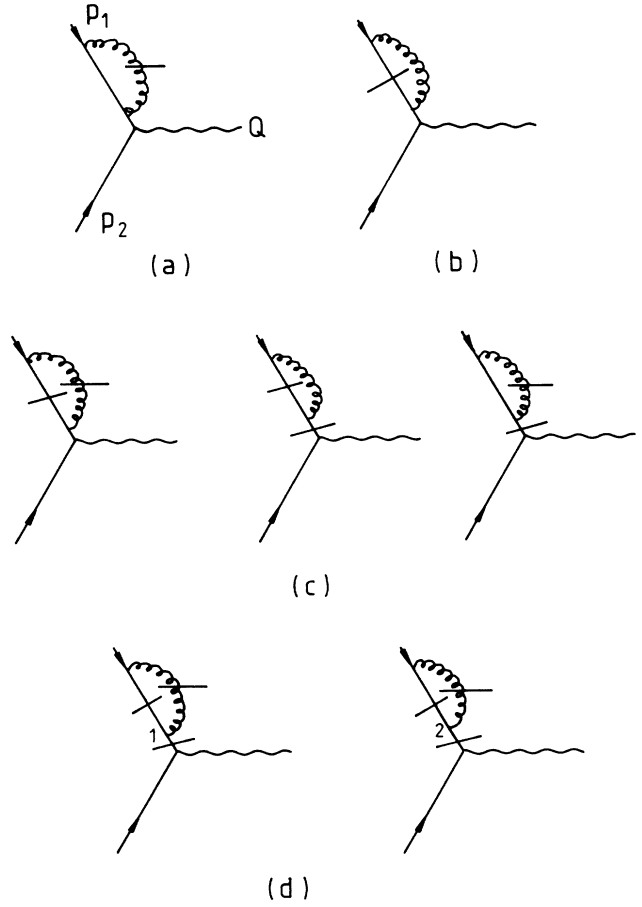

FIG. 5. Feynman diagrams for the temperature-dependent self-energy corrections.

and

$$I_2(\omega)=\int_{E_{\min}}^{E_{\max}}\frac{dE}{(E-Q/2)^2}$$
$$=\frac{4\kappa\left[1-\dfrac{4m^2}{Q(Q+2\omega)+\lambda^2}\right]^{1/2}}{\omega^2-\kappa^2\left[1-\dfrac{4m^2}{Q(Q+2\omega)+\lambda^2}\right]}, \qquad (3.15)$$

so that

$$I_1^S(\omega)=\ln\frac{\omega+\kappa v}{\omega-\kappa v} \qquad (3.16)$$

and

$$I_2^S(\omega)=\frac{4\kappa v}{\omega^2-\kappa^2 v^2}, \qquad (3.17)$$

with $v=(1-4m^2/Q^2)^{1/2}$.

Similarly we find, for the case of absorption,

$$R_{\rm abs}^S=-4\frac{\alpha_s}{\pi^2}N_C C_F\int_\lambda^{\omega_{\max}}d\omega\, n_B(\omega)n_F(Q/2)n_F(Q/2-\omega)\mathcal{E}_2, \qquad (3.18)$$

with

$$\mathcal{E}_2(\omega)=\mathcal{E}_1(-\omega). \qquad (3.19)$$

3. Detailed-balance relationships

In order to simplify Eqs. (3.12) and (3.18), namely, to keep only one statistical factor depending on ω, we use the following relationships:[18]

$$[1+n_B(\omega)]n_F(Q/2+\omega)=n_F(Q/2)[n_B(\omega)+n_F(Q/2+\omega)] \qquad (3.20)$$

and

$$n_B(\omega)n_F(Q/2-\omega)=n_F(Q/2)[1+n_B(\omega)-n_F(Q/2-\omega)], \qquad (3.21)$$

with $Q/2-\omega\geq 0$. These relations can be verified identically. They may be also obtained by applying detailed balance for the statistical factors on a given quark line with emission or absorption of a gluon. This leads then to

$$R_{\rm em}^S=-4\frac{\alpha_s}{\pi^2}N_C C_F n_F^2(Q/2)\int_\lambda^\infty d\omega[n_B(\omega)+n_F(Q/2+\omega)]\mathcal{E}_1 \qquad (3.22)$$

and

$$R_{\rm abs}^S=-4\frac{\alpha_s}{\pi^2}N_C C_F n_F^2(Q/2)\int_\lambda^{\omega_{\max}}d\omega[1+n_B(\omega)-n_F(Q/2+\omega)]\mathcal{E}_2. \qquad (3.23)$$

We rewrite the sum of these two terms as

$$R_{\rm em}^S+R_{\rm abs}^S=-4\frac{\alpha_s}{\pi^2}N_C C_F n_F^2(Q/2)\left[\int_\lambda^\infty d\omega\, n_B(\omega)(\mathcal{E}_1+\mathcal{E}_2)-\int_{\omega_{\max}}^\infty d\omega\, n_B(\omega)\mathcal{E}_2+\int_\lambda^{\omega_{\max}}d\omega\mathcal{E}_2\right.$$
$$\left.+\int_0^\infty d\omega\, n_F(Q/2+\omega)\mathcal{E}_1-\int_0^{\omega_{\max}}d\omega\, n_F(Q/2-\omega)\mathcal{E}_2\right]. \qquad (3.24)$$

Because of Eq. (3.19) the sum of the two terms in the last line of the above expression is not IR divergent. Keeping there only mass singular terms we may replace $\mathcal{E}_1$ and $\mathcal{E}_2$ by

$$\bar{\mathcal{E}}_1=-\tfrac{1}{2}Q^2\ln\frac{Q^2}{m^2}\left[\frac{1}{Q}+\frac{\omega}{Q^2}+\frac{1}{2\omega}\right],\quad \bar{\mathcal{E}}_2=\tfrac{1}{2}Q^2\ln\frac{Q^2}{m^2}\left[\frac{1}{Q}-\frac{\omega}{Q^2}-\frac{1}{2\omega}\right], \qquad (3.25)$$

respectively, since $I_1^S(\omega)\simeq\ln Q^2/m^2$ in the limit $\lambda\to 0$, $m\to 0$. This substitution is also allowed in the second term of Eq. (3.24); in addition we can replace everywhere $\omega_{\max}$ by $Q/2$.

4. Compton contribution

Performing similar steps which lead to Eq. (3.8) and keeping only the singular terms, only mass singularities, the Compton contribution [Fig. 2(c)] is found to be

$$R_{\rm Compton}=4\frac{\alpha_s}{\pi^2}N_C C_F\int_{Q/2}^\infty d\omega\, n_B(\omega)\int_{\bar{E}}^\infty dE\, n_F(E)[1-n_F(E+\omega-Q)]\left[\frac{1}{2Q(E-Q/2)}\left[-Q^2+Q\omega+\frac{Q^3}{2\omega}\right]\right], \qquad (3.26)$$

where scatterings off a quark and an antiquark are summed. Since the integration with respect to E extends now to infinity we safely isolate the mass singularity by expanding

$$n_F(E)[1-n_F(E+\omega-Q)]=e^{-\beta(E-Q/2)}n_F(Q/2)[1-n_F(\omega-Q/2)]+O(E-Q/2)\ . \tag{3.27}$$

The first term keeps the integral defined and the second one does not contain mass singular logarithms. In the limit $m\to 0$ we use the approximation

$$\int_{\bar{E}}^{\infty}\frac{e^{-\beta(E-Q/2)}}{E-Q/2}dE\simeq-\ln\left\{\frac{\beta\omega}{2}\left[\left[1+\frac{4m^2}{2\omega Q-Q^2}\right]^{1/2}-1\right]\right\}\simeq\ln\frac{Q^2}{m^2}-\ln\frac{\beta\omega Q}{2\omega-Q}\ . \tag{3.28}$$

Since $n_F(\omega-Q/2)$ is finite at $\omega=Q/2$ the contribution of the second term in Eq. (3.28) is integrable and leads to a nonsingular result; therefore it may be dropped. We then obtain

$$R^S_{\text{Compton}}=-4\frac{\alpha_s}{\pi^2}N_CC_Fn_F(Q/2)\int_{Q/2}^{\infty}d\omega\, n_B(\omega)[1-n_F(\omega-Q/2)]\bar{\mathcal{C}}_2\ . \tag{3.29}$$

Using the relationship, similar to Eqs. (3.20) and (3.21),

$$n_B(\omega)[1-n_F(\omega-Q/2)]=n_F(Q/2)[n_B(\omega)+n_F(\omega-Q/2)]\ , \tag{3.30}$$

for $\omega-Q/2\geq 0$, we find that the complete singular contribution of the real diagrams (Figs. 2 and 3) may be written as

$$\begin{aligned}R^S_{\text{real}}&=R^S_{\text{em}}+R^S_{\text{abs}}+R^S_{\text{Compton}}\\&=-4\frac{\alpha_s}{\pi^2}N_CC_Fn_F^2(Q/2)\left[\int_{\lambda}^{Q/2}d\omega\,\mathcal{C}_2+\int_{\lambda}^{\infty}d\omega\, n_B(\omega)(\mathcal{C}_1+\mathcal{C}_2)+\int_0^{\infty}d\omega\, n_F(Q/2+\omega)\bar{\mathcal{C}}_1\right.\\&\quad\left.-\int_0^{Q/2}d\omega\, n_F(Q/2-\omega)\bar{\mathcal{C}}_2+\int_{Q/2}^{\infty}d\omega\, n_F(\omega-Q/2)\bar{\mathcal{C}}_2\right]\ ,\end{aligned} \tag{3.31}$$

with $\mathcal{C}_1,\mathcal{C}_2$ given by Eqs. (3.13) and (3.19), and $\bar{\mathcal{C}}_1,\bar{\mathcal{C}}_2$ by Eq. (3.25), respectively.

B. Virtual diagrams

Virtual $O(\alpha_s)$ contributions to the dilepton rate come from the vertex corrections (Fig. 4) and from the self-energy insertions on external quark lines (Fig. 5).

A number of specific finite-T contributions, involving slashed propagators, turn out to be zero in the present regularization scheme. The triple slashed diagram of Fig. 4(e) yields a contribution of the type $\delta(t)\delta(u)$, which vanishes when the gluon has a nonzero mass λ as discussed in Sec. III A. The same is true for the diagrams of Fig. 4(d), which yield similar terms, since they only contribute through their imaginary part. The triple slashed self-energy diagrams of Fig. 5(d), which contain either a type-1 or a type-2 vertex, vanish for a nonzero gluon mass. The double slashed diagrams of Fig. 5(c) contributing only through their imaginary part also vanish. In other words the double slashed self-energy parts $\tilde{\Sigma}_{11}$ and $\tilde{\Sigma}_{12}$ are zero for on-shell quarks, when the gluon has a nonzero mass.

We now treat the nonvanishing virtual diagrams. The ultraviolet (UV) divergences are dealt with in the same way as at zero temperature. Because of the suppression role of the Fermi-Dirac and Bose-Einstein factors at large momenta, there are no additional UV divergences at finite temperature. Using on-shell renormalization one may ignore the $T=0$ fermion self-energy insertions, thus keeping only the finite contribution of the vertex correction known from QED (Refs. 19 and 20).

1. QED-like vertex correction

The UV finite contribution to the rate from the diagram of Fig. 4(a) is

$$R_a^{\text{vertex}}=\frac{1}{\pi}N_CC_Fn_F^2(Q/2)v[(Q^2+2m^2)\,\text{Re}F_1(Q)+3mQ^2\,\text{Re}F_2(Q)]\ , \tag{3.32}$$

where[20]

$$\text{Re}F_1(Q)=\frac{\alpha_s}{\pi}\left[\ln\frac{\lambda}{m}\left[\frac{1+v^2}{2v}\ln\frac{1+v}{1-v}-1\right]-1+\frac{1+2v^2}{4v}\ln\frac{1+v}{1-v}-\frac{1+v^2}{v}\int_0^{\ln[(1+v)/(1-v)]/2}d\phi\,\phi\coth\phi\right]+O(\lambda) \tag{3.33}$$

and

$$\text{Re}F_2(Q)=-\frac{\alpha_s}{2\pi}\frac{m}{Q^2}\frac{1}{v}\ln\frac{1+v}{1-v}\ . \tag{3.34}$$

The infrared and mass singular part of Eq. (3.32) comes only from $\mathrm{Re}F_1$, which is

$$\mathrm{Re}F_1(Q)\simeq\frac{\alpha_s}{\pi}\left[\ln\frac{\lambda}{m}\left[\frac{1+v^2}{2v}\ln\frac{1+v}{1-v}-1\right]-\frac{1}{4}\ln\frac{Q^2}{m^2}\left[\ln\frac{Q^2}{m^2}-3\right]\right] . \tag{3.35}$$

Here and in the following terms of $O(m^2\ln Q^2/m^2)$ are consistently neglected, whereas terms of $O(m^2\ln\lambda/m)$ are kept in order to check the IR cancellation at finite values of m (Ref. 21).

2. *Finite-temperature vertex corrections*

The finite-temperature vertex correction associated with the thermal gluon propagator [Fig. 4(b)] takes the form

$$R_b^{\text{vertex}}\simeq-\frac{\alpha_s}{\pi^3}N_C C_F n_F^2(Q/2)v(Q^4-4m^4)\int d^4k\, n_B(k)\delta(k^2-\lambda^2)\frac{1}{(2k\cdot p_1+\lambda^2)(2k\cdot p_2-\lambda^2)} , \tag{3.36}$$

neglecting terms in the trace which do not lead to singular terms. The integral in Eq. (3.36) is IR and mass singular. It is worked out in Appendix A and yields, keeping the singular part,

$$R_b^{\text{vertex}}\simeq-\frac{\alpha_s}{\pi^2}N_C C_F n_F^2(Q/2)(Q^2+2m^2)(1+v^2)I_S . \tag{3.37}$$

The contribution coming from diagrams with one slashed quark propagator [Fig. 4(c)] is written as

$$R_c^{\text{vertex}}\simeq-2\frac{\alpha_s}{\pi^3}N_C C_F n_F^2(Q/2)Q^4\,\mathrm{Re}\int d^4l\, n_F(l)\delta(l^2-m^2)\frac{1}{(p_1-l)^2[(Q-l)^2-m^2+i\varepsilon]} , \tag{3.38}$$

again keeping only mass singular parts; there are no IR divergences. This then leads to R_c^{vertex} in terms of a principal-value integral:

$$R_c^{\text{vertex}}\simeq-2\frac{\alpha_s}{\pi^2}N_C C_F n_F^2(Q/2)Q^2\ln\frac{Q^2}{m^2}P\int\frac{l\,dl}{l^2-Q^2/4}n_F(l) . \tag{3.39}$$

3. *Finite-temperature self-energy corrections*

We first consider the diagram of Fig. 5(a) and calculate the corresponding self-energy insertion

$$\Sigma_T^G(p)=\frac{\alpha_s}{\pi^2}\int d^4k\, n_B(k)\delta(k^2-\lambda^2)\frac{\not p-\not k-2m}{(p-k)^2-m^2+i\varepsilon} . \tag{3.40}$$

Only the real part contributes to the rate. Following Ref. 6 we expand the integrand around $\not p=m$. With the expansion of the denominator

$$\frac{1}{(p-k)^2-m^2}\simeq\frac{1}{-2p\cdot k+\lambda^2}\bigg|_{p^2=m^2}-(p^2-m^2)\frac{1-k_0/p_0}{(-2p\cdot k+\lambda^2)^2}\bigg|_{p^2=m^2} , \tag{3.41}$$

we obtain

$$\mathrm{Re}\Sigma_T^G(p)=\frac{\alpha_s}{\pi^2}[(\not p-m)I_A+\not I\,|_{\not p=m}+(p^2-m^2)\not L\,|_{\not p=m}+\cdots] , \tag{3.42}$$

where m denotes the $T=0$ renormalized mass. The integrals I_A, I^μ, and L^μ are given in Appendix A. Here we only remark that the temperature-dependent integral I_A, as I_S in Eq. (3.37), is IR as well as mass singular (Appendix A), and we note the relation

$$L\cdot p=-\frac{I_0}{2E_p} , \tag{3.43}$$

with $E_p=\sqrt{\mathbf{p}^2+m^2}$. Furthermore the quark momentum p is identified either with p_1 or with p_2 (Fig. 1), so that $E_p=Q/2$ in the special kinematical configuration we are considering.

We now turn to the diagrams of Fig. 5(b) with one slashed quark line. The corresponding self-energy is

$$\Sigma_T^q(p)=\frac{\alpha_s}{\pi^2}\int d^4l\, n_F(l)\delta(l^2-m^2)\frac{\not l+2m}{(p+l)^2+i\varepsilon} , \tag{3.44}$$

putting $k=p+l$. Performing an expansion similar to Eq. (3.41) we derive

$$\mathrm{Re}\Sigma_T^q(p)=\frac{\alpha_s}{\pi^2}[2mJ_A+\boldsymbol{J}\mid_{\not p=m}+(p^2-m^2)\not K\mid_{\not p=m}]\ , \tag{3.45}$$

with the integrals J_A, J^μ, and K^μ of Appendix A. A useful relation similar to Eq. (3.43) holds in the limit $m\to 0$:

$$K\cdot p\simeq -\frac{J_0}{2E_p}\ . \tag{3.46}$$

We adopt in this section the procedure of Donoghue and co-workers[6] to handle the finite mass and wave-function renormalization associated with $\Sigma_T=\Sigma_T^G+\Sigma_T^q$. Counterterms proportional to $\boldsymbol{I}$, Eq. (3.42), and to $\boldsymbol{J}$, Eq. (3.45), are introduced to carry out the mass renormalization, so that in the following the mass m denotes the quark mass at $T\neq 0$. The temperature-dependent renormalization constant Z_2 is found to be

$$Z_2^{-1}=1+\frac{\alpha_s}{\pi^2}C_F\left[-I_A+\frac{I_0}{E_p}+\frac{J_0}{E_p}\right]\ , \tag{3.47}$$

when only IR and mass singular terms are taken into account.

With the properly defined counterterm added we find the sum of the amplitudes of the self-energy diagrams [Figs. 5(a) and 5(b)], including the crossed ones, given by

$$M_\mu^{\mathrm{CT}}+M_\mu^{\mathrm{SE}}=\frac{\alpha_s}{\pi^2}C_F\left[2I_A-2\frac{I_0}{E_p}-2\frac{J_0}{E_p}\right]M_\mu^{\mathrm{Born}}\ . \tag{3.48}$$

After dividing this amplitude by $\sqrt{Z_2}$ for each external quark line we find the following contribution to the rate:

$$R^{\mathrm{SE}}=\frac{\alpha_s}{\pi^3}N_C C_F n_F^2(Q/2)v(Q^2+2m^2)\left[I_A-\frac{I_0}{E_p}-\frac{J_0}{E_p}\right]\ , \tag{3.49}$$

which we may cast into

$$R^{\mathrm{SE}}=\frac{\alpha_s}{\pi^2}N_C C_F n_F^2(Q/2)\left[v(Q^2+2m^2)\frac{I_A}{\pi}-4\ln\frac{Q^2}{m^2}(I_B+I_F)\right]\ , \tag{3.50}$$

performing consistently the limits $m,\lambda\to 0$ (cf. Appendix A).

C. Cancellations

We are now in the position to see explicitly how the cancellations take place among the various singular pieces.

In order to make the cancellation of singularities more transparent we rewrite the contributions of real diagrams R^S_{real} of Eq. (3.31) in terms of the integrals defined in Appendix A. We note that the first integral does not depend on the temperature and it may be performed explicitly in the limit $m,\lambda\to 0$ (Ref. 22). Following the order of the integrals in Eq. (3.31) we obtain[21]

$$\begin{aligned}R^S_{\mathrm{real}}=\frac{\alpha_s}{\pi^2}N_C C_F n_F^2(Q/2)\Bigg[&v(Q^2+2m^2)\left[1-\frac{1+v^2}{2v}\ln\frac{1+v}{1-v}\right]\ln\frac{\lambda}{m}+\frac{1}{4}Q^2\ln\frac{Q^2}{m^2}\left[\ln\frac{Q^2}{m^2}-3\right]\\&+\left[(Q^2+2m^2)(1+v^2)I_S-v(Q^2+2m^2)\frac{I_A}{\pi}+4\ln\frac{Q^2}{m^2}I_B\right]\\&+\left[2Q^2\ln\frac{Q^2}{m^2}P\int\frac{l\,dl}{l^2-Q^2/4}n_F(l)+4\ln\frac{Q^2}{m^2}I_F\right]\Bigg]\ .\end{aligned} \tag{3.51}$$

The principal-value integral [cf. Eq. (3.39)] is equal to

$$P\int\frac{l\,dl}{l^2-Q^2/4}n_F(l)\equiv\frac{1}{2}\left[\int_0^{Q/2}\frac{d\omega}{\omega}[n_F(\omega+Q/2)-n_F(Q/2-\omega)]+\int_{Q/2}^{\infty}\frac{d\omega}{\omega}[n_F(\omega+Q/2)+n_F(\omega-Q/2)]\right]\ , \tag{3.52}$$

which may be verified with an obvious change of variables. The terms in the last two square brackets in R^{S}_{real} cancel exactly against the sum of the two vertex contributions R_b^{vertex}, Eq. (3.37), and R_c^{vertex}, Eq. (3.39), and of the self-energy term R^{SE}, Eq. (3.50), respectively. This cancellation may be considered as the genuine finite-temperature cancellation of IR and mass singularities up to $O(\alpha_s)$, including the temperature-dependent IR singularities in the integrals I_A and I_S which are not present at $T=0$. The remaining cancellation of the first term in Eq. (3.51) against the vertex term R_a^{vertex}, Eqs. (3.32)–(3.35), is, apart from the factor $n_F^2(Q/2)$, familiar from the $O(\alpha_s)$ QCD calculation for the cross section $\sigma(e^+e^-\to\text{hadrons})$, which is known to be free of IR and mass singularities. Here it can be viewed as a consistency check of our calculation.

In summary the dilepton production rate up to $O(\alpha_s)$ is infrared safe and free of mass singularities in the limit of $m,\lambda\to 0$ (Refs. 23–25).

IV. DILEPTON RATE AND THE THERMAL VACUUM-POLARIZATION TENSOR

In perturbative field theory at zero temperature, cross sections and rates of physical processes may be related to discontinuities of self-energy functions. A well-known example, relevant for our further discussion, is the total hadronic e^+e^- annihilation cross section at high energies, which is proportional to the absorptive part of the vacuum-polarization tensor,

$$\Pi^{\mu\nu}(Q)=i\int d^4x\, e^{-iQ\cdot x}\langle 0\,|\,TJ^{\mu}(x)J^{\nu}(0)\,|\,0\rangle\ . \tag{4.1}$$

In this section we conjecture similar relations to hold at finite temperature. Especially we explore the connection between the dilepton production rate at finite temperature and the vacuum-polarization tensor for $T\neq 0$, having in mind to exploit the relation between $\langle W^{\mu\nu}(Q)\rangle$, Eq. (2.22), and the thermal vacuum-polarization tensor

$$\langle\Pi^{\mu\nu}(Q)\rangle\equiv i\int d^4x\, e^{-iQ\cdot x}\langle 0(\beta)\,|\,TJ^{\mu}(x)J^{\nu}(0)\,|\,0(\beta)\rangle\ . \tag{4.2}$$

In this way we try to generalize the suggestions and (one-loop) results of Weldon[11] and Kobes and Semenoff[12,13] to the case of external electromagnetic currents. At the same time we extend this type of calculations to the two-loop level.

In order to perform the perturbative QCD calculation of $\langle\Pi^{\mu\nu}(Q)\rangle$ up to $O(\alpha_s)$, we first introduce the formal notion of type-1 and -2 photon fields and the corresponding type-1 and -2 vertices for their couplings to quarks, although the heavy photon in the dilepton production process is not thermalized. Apart from the color structure, these vertices are treated on the same level as the QCD type-1 and -2 quark-gluon vertices. Treating for the moment photons as thermalized, together with the quarks and gluons, one may introduce the finite temperature 2×2 full photon Green's function $\mathcal{D}_{ab}$ in analogy to the full quark propagator. It satisfies a Schwinger-Dyson equation similar to Eq. (2.18), in which the photon self-energy matrix Π_{ab} plays the role of Σ_{ab}. Suppressing Lorentz indices it is

$$i\mathcal{D}_{ab}=U(\beta,Q)\begin{bmatrix}\mathcal{D}(Q) & 0\\ 0 & \mathcal{D}^*(Q)\end{bmatrix}U(\beta,Q)\ , \tag{4.3}$$

with the U matrix of Eq. (2.10) and where

$$\mathcal{D}(Q)=\frac{i}{Q^2[1+\tilde{\Pi}(Q)]+i\varepsilon}\ , \tag{4.4}$$

in analogy to the fermion case in Eq. (2.20). The complex photon self-energy function $\tilde{\Pi}(Q)$ is related to the trace of $\langle\Pi^{\mu\nu}_{ab}(Q)\rangle$, which we denote by $\tilde{\Pi}_{ab}$, interpreting the indices (a,b) as the ones corresponding to the type of the photon field or equivalently to the type of the photon-quark coupling. According to Refs. 12 and 13 the relevant quantity connected to rates is $\text{Im}\tilde{\Pi}$, which we calculate from the photon self-energy matrix $\tilde{\Pi}_{ab}$, using the relations

$$\text{Re}\tilde{\Pi}=\text{Re}\tilde{\Pi}_{11}\ , \tag{4.5}$$

$$\text{Im}\tilde{\Pi}=\tanh\tfrac{1}{2}\beta Q_0\,\text{Im}\tilde{\Pi}_{11}=i\sinh\tfrac{1}{2}\beta Q_0\tilde{\Pi}_{12}\ , \tag{4.6}$$

valid for a timelike photon, $Q_0>0$. These relations are a consequence of the Schwinger-Dyson equation for the full photon propagator and its representation given by Eqs. (4.3) and (4.4). The diagrams for $\tilde{\Pi}_{12}$ in the one- and two-loop approximation with respect to QCD interactions are shown in Figs. 6–8. They are topologically the same as for the $T=0$ calculation of $\Pi^{\mu\nu}(Q)$, Eq. (4.1), however, at $O(\alpha_s)$ the number of graphs increases because of the two types of quark-gluon vertices present at $T\neq 0$.

Instead of giving a general proof we proceed by first evaluating the one-loop approximation, which we then compare with the result already obtained for R^{Born} in Sec. II; this provides the detailed identification of the rate R with $\text{Im}\tilde{\Pi}$. Next we generalize to the two-loop calculation and we finally find the same results as already derived in Sec. III. *A posteriori* this then justifies the approach of calculating the dilepton rate at finite temperature from the absorptive part of the thermal vacuum-

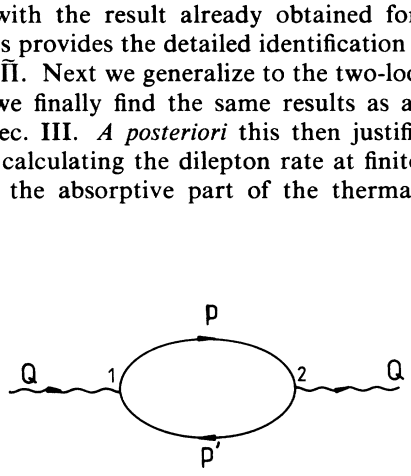

FIG. 6. One-loop vacuum-polarization graph for the calculation of $\tilde{\Pi}_{12}$ at $T\neq 0$. The quark propagators [Eq. (2.17)] include the temperature dependence.

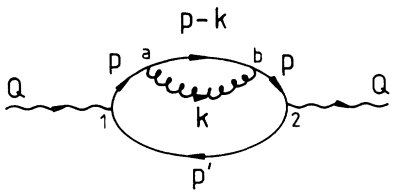

FIG. 7. Two-loop photon polarization graph for the calculation of $\tilde{\Pi}_{12}^{\mathrm{SE}}$. The labels $a,b=1,2$ denote the type of the quark-gluon vertex.

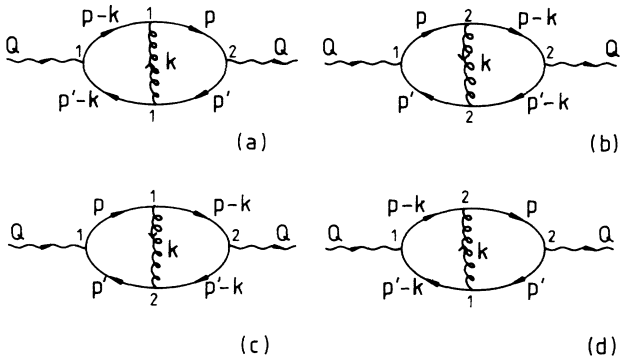

FIG. 8. Two-loop photon polarization graphs for the calculation of $\tilde{\Pi}_{12}^{\mathrm{VI}}$ and $\tilde{\Pi}_{12}^{\mathrm{VII}}$.

polarization tensor. Before entering the detailed calculation we add the obvious remark that in this approach only thermal Green's functions are involved in contrast with the amplitude approach, which in addition requires knowledge of thermal spinors.[6]

A. One-loop approximation

It is straightforward to derive the one-loop expression for $\tilde{\Pi}_{12}$. With the momentum labels indicated in Fig. 6 this quark-loop, with the temperature-dependent fermion propagators of Eq. (2.17), reads

$$i\tilde{\Pi}_{12}=N_C\int\frac{d^4p}{(2\pi)^4}i\tilde{S}_{12}(p)i\tilde{S}_{21}(p')\times\mathrm{Tr}[\gamma^\mu(\not p+m)\gamma_\mu(\not p'+m)]\ , \tag{4.7}$$

with $p'=p-Q$. Substituting the expressions for $\tilde{S}_{12}$ and $\tilde{S}_{21}$, respectively, we obtain

$$i\tilde{\Pi}_{12}=-N_C\int\frac{d^4p}{(2\pi)^4}\tfrac{1}{2}\sin 2\phi_p\tfrac{1}{2}\sin 2\phi_{p'}\epsilon(p_0)\epsilon(p_0')\delta(p^2-m^2)\delta(p'^2-m^2)\mathrm{Tr}[\gamma^\mu(\not p+m)\gamma_\mu(\not p'+m)]\ . \tag{4.8}$$

Working out the δ-function constraints for positive photon energy Q_0 it follows, from Eq. (4.6), that

$$\mathrm{Im}\tilde{\Pi}=-\frac{N_C}{2}(Q^2+2m^2)[1-\exp(\beta Q_0)]\int\frac{d^3p}{(2\pi)^2E_1E_2}\delta(Q_0-E_1-E_2)n_F(E_1)n_F(E_2)\ , \tag{4.9}$$

where

$$E_1=\sqrt{\mathbf{p}^2+m^2}\ , \tag{4.10}$$

$$E_2=\sqrt{(\mathbf{p}-\mathbf{Q})^2+m^2}\ . \tag{4.11}$$

Applying the identity for the n_F distribution

$$e^{\beta E}n_F(E)=1-n_F(E)\ , \tag{4.12}$$

$\mathrm{Im}\tilde{\Pi}$ may be decomposed into two terms:

$$\mathrm{Im}\tilde{\Pi}=\frac{N_C}{2}(Q^2+2m^2)\int\frac{d^3p}{(2\pi)^2E_1E_2}\delta(Q_0-E_1-E_2)\{[1-n_F(E_1)][1-n_F(E_2)]-n_F(E_1)n_F(E_2)\}\ . \tag{4.13}$$

The same result is derived when taking the discontinuity of $\tilde{\Pi}_{11}$ in Eq. (4.6). This way of performing the calculation is, however, more cumbersome.

We identify[11] the two terms in Eq. (4.13) as the production rate R, Eq. (2.23), and the annihilation (decay) rate R_D of the heavy photon, respectively:

$$2\,\mathrm{Im}\tilde{\Pi}\equiv R_D-R\ . \tag{4.14}$$

The two rates are related by

$$R_D=e^{\beta Q_0}R\ , \tag{4.15}$$

which follows from Eq. (4.12). For the photon at rest R indeed coincides with R^{Born}, Eq. (2.31). Although the annihilation process, $\gamma^*\to q\bar{q}$, is not easy to realize experimentally at $T\neq 0$, it is instructive to investigate the zero-temperature limit of $\mathrm{Im}\tilde{\Pi}$ and R_D, respectively. For $\beta\to\infty$, n_F vanishes and from Eq. (4.13) we recover that $\mathrm{Im}\tilde{\Pi}$ becomes proportional to the Born approximation of the cross section for $e^+e^-\to$hadrons, when $Q^\mu=(Q,\mathbf{0})$. For this process the $O(\alpha_s)$ QCD corrections[26,27] are known, and therefore we expect

$$R_D\simeq\frac{1}{2\pi}N_CQ^2\left[1+\frac{3}{4}C_F\frac{\alpha_s}{\pi}+O(\alpha_s^2)\right]\ , \tag{4.16}$$

for $Q^2\gg 4m^2$ and $\beta\to\infty$. From this and with Eq. (4.15), we have some indications for small QCD corrections of

the production rate R for large values of β as long as α_s behaves smoothly with respect to T.

In the following we assume that the relations, Eqs. (4.14) and (4.15), remain valid at the two-loop level, which then allows us to calculate R from $\mathrm{Im}\tilde{\Pi}$ or $\tilde{\Pi}_{12}$, respectively:

$$R \equiv \frac{2\,\mathrm{Im}\tilde{\Pi}}{e^{\beta Q_0}-1} = \exp(-\tfrac{1}{2}\beta Q_0) i\tilde{\Pi}_{12} \ . \tag{4.17}$$

However, it is most convenient to use $\tilde{\Pi}_{12}$ for the explicit calculation at the two-loop level.

B. Two-loop approximation

At order α_s the calculation of $\tilde{\Pi}_{12}$ involves the two topologically different two-loop diagrams: namely, the self-energy (Fig. 7) and vertex-type (Fig. 8) graphs, respectively.

We start to discuss the former ones, where one first calculates the $O(\alpha_s)$ correction δS_{ab} to the free quark propagators $S_{12}(p)$ and $S_{21}(p')$. This is done with the help of the Schwinger-Dyson equation, Eq. (2.18):

$$i\delta S_{12}(p) = \sum_{a,b=1,2} iS_{1a}(p)[-i\Sigma_{ab}(p)]iS_{b2}(p) \ . \tag{4.18}$$

One has to remark that the four terms in Eq. (4.18) are ill defined separately, because each of them contains a product of δ functions with the same argument: namely, $[\delta(p^2-m^2)]^2$. However, after summation $\delta S_{12}(p)$ becomes well defined, since all these singular terms cancel. The result is

$$i\delta S_{12}(p) = -\epsilon(p_0)\sin 2\phi_p \,\mathrm{Re}\{S(p)[-i\Sigma(p)]S(p)\} \ , \tag{4.19}$$

where the fermion self-energy function $\Sigma(p)$ for $T\neq 0$ satisfies the conditions[12]

$$\mathrm{Re}\Sigma(p) = \mathrm{Re}\Sigma_{11}(p) \ , \tag{4.20}$$

$$\mathrm{Im}\Sigma(p) = \epsilon(p_0)\coth(\tfrac{1}{2}\beta p_0)\,\mathrm{Im}\Sigma_{11} = -i\epsilon(p_0)\cosh(\tfrac{1}{2}\beta p_0)\Sigma_{12} \ , \tag{4.21}$$

which follow from Eqs. (2.18)–(2.20). The result in Eq. (4.19) is rederived in Appendix B, because it is the most elegant way to prove, independently of the regularization method (cf. the discussion in Sec. III), that the rate R is free of pinch singularities. Thus it represents one of the main advantages in favor of the discontinuity approach.

Inserting Eq. (4.19) into $\tilde{\Pi}_{12}$ we obtain the self-energy contribution (Fig. 7)

$$i\tilde{\Pi}_{12}^{\mathrm{SE}} = -2N_C C_F \int \frac{d^4p}{(2\pi)^3}\tfrac{1}{2}\sin 2\phi_p \tfrac{1}{2}\sin 2\phi_{p'}\epsilon(p_0)\epsilon(p_0')\delta(p'^2-m^2)\mathrm{Tr}(\gamma^\mu \mathrm{Re}\{S(p)[-i\Sigma(p)]S(p)\}\gamma_\mu(\not{p}'+m)) \ . \tag{4.22}$$

An analogous expression has to be added in order to include the self-energy correction of the quark propagator with momentum $p'=p-Q$.

Concerning the vertex-type corrections, it turns out that it is convenient to attach different momentum labels on the internal quark lines, and to sum the four contributions (Fig. 8) in pairs. We first consider the diagrams of Figs. 8(a) and 8(b). Using the cyclic property of the trace we find

$$\begin{aligned} i\tilde{\Pi}_{12}^{\mathrm{VI}} = 4\pi\alpha_s N_C C_F \int \frac{d^4p\,d^4k}{(2\pi)^8} & i\tilde{S}_{12}(p)i\tilde{S}_{21}(p')\{iD_{11}(k)i\tilde{S}_{11}(p-k)i\tilde{S}_{11}(p'-k)+iD_{22}(k)i\tilde{S}_{22}(p-k)i\tilde{S}_{22}(p'-k)\} \\ & \times \mathrm{Tr}[\gamma^\mu(\not{p}-\not{k}+m)\gamma^\nu(\not{p}+m)\gamma_\mu(\not{p}'+m)\gamma_\nu(\not{p}'-\not{k}'+m)] \ , \end{aligned} \tag{4.23}$$

choosing the Feynman gauge for the gluon propagator given in Eqs. (2.8)–(2.12). Because of the relations $iD_{22}=(iD_{11})^*$ and $i\tilde{S}_{22}=(i\tilde{S}_{11})^*$ the expression in the curly brackets is identical to

$$\{\ \} = 2\,\mathrm{Re}[iD_{11}(k)i\tilde{S}_{11}(p-k)i\tilde{S}_{11}(p'-k)] \ . \tag{4.24}$$

In a similar way we sum the terms corresponding to Figs. 8(c) and 8(d):

$$\begin{aligned} i\tilde{\Pi}_{12}^{\mathrm{VII}} = -4\pi\alpha_s N_C C_F \int \frac{d^4p\,d^4k}{(2\pi)^8} & iD_{12}(k)i\tilde{S}_{12}(p-k)i\tilde{S}_{21}(p')2\,\mathrm{Re}[i\tilde{S}_{11}(p)i\tilde{S}_{22}(p'-k)] \\ & \times \mathrm{Tr}[\gamma^\mu(\not{p}+m)\gamma^\nu(\not{p}-\not{k}+m)\gamma_\mu(\not{p}'-\not{k}+m)\gamma_\nu(\not{p}'+m)] \ . \end{aligned} \tag{4.25}$$

The total $O(\alpha_s)$ correction to the dilepton production rate R is the sum of the above terms: namely,

$$R = \exp(-\tfrac{1}{2}\beta Q_0)(2i\tilde{\Pi}^{\mathrm{SE}}_{12} + i\tilde{\Pi}^{\mathrm{VI}}_{12} + i\tilde{\Pi}^{\mathrm{VII}}_{12}) , \tag{4.26}$$

which has to be evaluated for $Q_0 > 0$ above the threshold $Q^2 \geq 4m^2$.

C. Explicit two-loop calculation

As in the previous section also here our main emphasis is the IR and mass singularities. Again R, Eq. (4.26), is explicitly calculated for the heavy photon at rest. First we briefly discuss the UV renormalization, because the terms $\tilde{\Pi}^{\mathrm{SE}}_{12}$ and $\tilde{\Pi}^{\mathrm{VI}}_{12}$ are UV divergent.

1. UV divergencies and mass renormalization

Since the UV divergences are the same as at zero temperature we perform the renormalization at $T=0$ ("T_0" renormalization[17]). Contrary to the treatment in Sec. III no temperature-dependent renormalization constants and mass counterterms are introduced. Therefore in this scheme one can follow the standard on-shell renormalization procedure.[19,20]

Keeping only the temperature-independent terms in the propagators, the UV-divergent parts of $\tilde{\Pi}^{\mathrm{SE}}_{12}$, Eq. (4.22), and of $\tilde{\Pi}^{\mathrm{VI}}_{12}$, Eq. (4.23), exactly cancel, because of the $T=0$ Ward identity.[12] Therefore $\mathrm{Im}\tilde{\Pi}$ and consequently R are UV finite, which is a consequence of the fact that the photon self-energy tensor is renormalized by subtraction as it is known from the QCD calculation for $e^+e^- \to$ hadrons.[27] The remaining QED-like finite part becomes, after the limit $m, \lambda \to 0$ is taken,

$$\begin{aligned} 2i\tilde{\Pi}^{\mathrm{SE}}_{12} + i\tilde{\Pi}^{\mathrm{VI}}_{12} \to{}& 2N_C C_F \,\mathrm{Re}F_1(Q) \\ &\times \int \frac{d^4p}{(2\pi)^4} i\tilde{S}_{12}(p) i\tilde{S}_{21}(p') \\ &\times \mathrm{Tr}[\gamma^\mu(\not{p}+m)\gamma_\mu(\not{p}'+m)] , \end{aligned} \tag{4.27}$$

and the corresponding correction to R agrees with R_a^{vertex} as given by Eqs. (3.32)–(3.35), when the photon is at rest.

2. Contribution from $\mathrm{Re}\Sigma_T$: thermal self-energy insertions

We continue in the $T=0$ renormalization scheme and evaluate the $T\neq 0$ part of $\tilde{\Pi}^{\mathrm{SE}}_{12}$ now considering the temperature-dependent terms of $\Sigma(p)$. Here we calculate the contribution due to $\mathrm{Re}\Sigma_T$, which is given by adding Eqs. (3.40) and (3.44):

$$\mathrm{Re}\Sigma_T(p) = \mathrm{Re}[\Sigma_T^G(p) + \Sigma_T^q(p)] . \tag{4.28}$$

We recall that $\mathrm{Re}\Sigma_T$ appears in the expression $\mathrm{Re}\{S(p)[-i\,\mathrm{Re}\Sigma_T(p)]S(p)\}$. Therefore we expand $(\not{p}+m)\,\mathrm{Re}\Sigma_T(p)(\not{p}+m)$ in powers of (p^2-m^2). With the same expansions [cf. Eq. (3.41)] as used in the previous section, and collecting the nonvanishing terms we find

$$\begin{aligned} \mathrm{Re}\{S(p)[-i\,\mathrm{Re}\Sigma_T(p)]S(p)\} = \frac{\alpha_s}{\pi}\delta(p^2-m^2) &\left[\int d^4k\, n_B(k)\delta(k^2-\lambda^2) \left[\frac{2m^2(\not{p}+m)}{(2p\cdot k-\lambda^2)^2} - \frac{\not{k}}{2p\cdot k-\lambda^2} \right] \right. \\ &\left. - \int d^4l\, n_F(l)\delta(l^2-m^2) \left[\frac{2m^2(\not{p}+m)(1+l_0/p_0)}{(2p\cdot l+2m^2)^2} + \frac{\not{p}+\not{l}-m}{2p\cdot l+2m^2} \right] \right] \\ &- m\Delta m(T)(\not{p}+m)\frac{\partial}{\partial p^2}\delta(p^2-m^2) , \end{aligned} \tag{4.29}$$

noting that $\mathrm{Re}\tilde{S}(p) = \pi\delta(p^2-m^2)$ and $\mathrm{Re}[i\tilde{S}(p)\tilde{S}(p)] = \pi\partial/\partial p^2\delta(p^2-m^2)$. The temperature-dependent mass shift $\Delta m(T)$, already given in Refs. 6 and 28, is

$$\Delta m(T) = \alpha_s C_F \frac{\pi T^2}{3m} + 2\alpha_s C_F \frac{1}{\pi m}\int_0^\infty \frac{l\,dl}{E_l} n_F(E_l) \left[l + \frac{m^2}{2|\mathbf{p}|} \ln\left[\frac{l-|\mathbf{p}|}{l+|\mathbf{p}|} \right] \right] , \tag{4.30}$$

with $E_l = \sqrt{l^2+m^2}$. In the limit of vanishing quark mass m the thermal mass becomes momentum independent:

$$m^2(T) = \pi\alpha_s C_F T^2 . \tag{4.31}$$

Next we insert Eq. (4.29) into Eq. (4.22) and with the integrals of Appendix A we derive, for the photon at rest, the same contribution to the rate as given by R^{SE} in Eq. (3.50), when only the IR and mass singular terms are kept. The thermal mass term proportional to $\partial/\partial p^2\delta(p^2-m^2)$ in Eq. (4.29) does not give rise to any singularities.

3. Contribution from $\tilde{\Pi}^{VI}_{12}$: the thermal vertex

Starting from the definition of the vertex correction $\tilde{\Pi}^{\mathrm{VI}}_{12}$, Eqs. (4.23) and (4.24), we obtain, besides the $T=0$ vertex term already discussed above, a thermal contribution to the rate. We first observe that the product of propagators in Eq. (4.24), when the temperature-dependent terms are considered, becomes

$$2\,\mathrm{Re}[iD_{11}(k)i\tilde{S}_{11}(p-k)i\tilde{S}_{11}(p'-k)]\to 4\pi n_B(k)\delta(k^2-\lambda^2)\,\mathrm{Re}[\tilde{S}(p-k)\tilde{S}(p'-k)]$$
$$-4\pi n_F(p-k)\delta((p-k)^2-m^2)\,\mathrm{Re}[D(k)\tilde{S}(p'-k)]$$
$$-4\pi n_F(p'-k)\delta((p'-k)^2-m^2)\,\mathrm{Re}[D(k)\tilde{S}(p-k)]\ , \tag{4.32}$$

since terms proportional to

$$\delta(k^2-\lambda^2)\delta((p-k)^2-m^2)\delta((p'-k)^2-m^2) \tag{4.33}$$

are omitted for kinematical reasons. They give a vanishing contribution to $\tilde{\Pi}_{12}^{\mathrm{VI}}$ for on-shell quarks, $p^2=p'^2=m^2$, and for $\lambda\neq 0$.

When the photon is at rest we work out the integrations with the help of Appendix A and we finally find the sum of the vertex contributions $R_b^{\mathrm{vertex}}+R_c^{\mathrm{vertex}}$ with the IR and mass singular behavior as given in Eqs. (3.37) and (3.39) of the previous section.

4. *Contributions from Im Σ and $\tilde{\Pi}_{12}^{VII}$: real gluon processes*

With the relation between the imaginary part of Σ and Σ_{12}, Eq. (4.21), we obtain, at $O(\alpha_s)$,

$$\mathrm{Im}\Sigma(p)=-8\pi\alpha_s\frac{\epsilon(p_0)}{\sin 2\phi_p}\int\frac{d^4k}{(2\pi)^4}i\tilde{S}_{12}(p-k)iD_{21}(k)(2m-\not{p}+\not{k})\ . \tag{4.34}$$

Inserting this expression into $\tilde{\Pi}_{12}^{\mathrm{SE}}$, Eq. (4.22), we find the contribution

$$i\tilde{\Pi}'_{12}=8\pi\alpha_s N_C C_F\int\frac{d^4p\,d^4k}{(2\pi)^5}\tfrac{1}{2}\sin 2\phi_{p'}\tfrac{1}{2}\sin 2\phi_{p-k}\tfrac{1}{2}\sinh 2\theta_k\epsilon(p'_0)\epsilon(p_0-k_0)$$
$$\times\delta(p'^2-m^2)\delta(k^2-\lambda^2)\delta((p-k)^2-m^2)\frac{1}{(p^2-m^2)^2}$$
$$\times\mathrm{Tr}[\gamma^\mu(\not{p}+m)(2m-\not{p}+\not{k})(\not{p}+m)\gamma_\mu(\not{p}'+m)]\ . \tag{4.35}$$

We encounter the same thermal phase-space integral as in the vertex correction $\tilde{\Pi}_{12}^{\mathrm{VII}}$, Eq. (4.25). Therefore it is convenient to add these two contributions, keeping in mind the additional self-energy correction, which we denote by $\tilde{\Pi}''_{12}$ and which is due to the insertion $\mathrm{Im}\Sigma(p')$ on the quark line with momentum p'. In order to evaluate the sum, actually corresponding to the real gluon processes

$$i\tilde{\Pi}_{12}^{\mathrm{real}}=i\tilde{\Pi}'_{12}+i\tilde{\Pi}''_{12}+i\tilde{\Pi}_{12}^{\mathrm{VII}}\ , \tag{4.36}$$

we note that the phase-space integral of $\tilde{\Pi}''_{12}$ may be transformed into the one of $\tilde{\Pi}'_{12}$ by substituting, $p'\to-(p'-k)$ and $p\to-(p-k)$. In $\tilde{\Pi}_{12}^{\mathrm{VII}}$ we replace $\mathrm{Re}[i\tilde{S}_{11}(p)i\tilde{S}_{22}(p'-k)]$ by $\mathrm{Re}[i\tilde{S}(p)i\tilde{S}(p'-k)]$, because terms similar to those of Eq. (4.33) are dropped for the same kinematical reason. Furthermore we decompose this propagator product into

$$\mathrm{Re}[\tilde{S}(p)\tilde{S}(p'-k)]=-\frac{1}{2Q\cdot k}\left[\frac{1}{p^2-m^2}+\frac{1}{(p'-k)^2-m^2}\right]\ , \tag{4.37}$$

taking into account the phase-space constraints in Eq. (4.35). Carrying through the necessary algebra we obtain

$$i\tilde{\Pi}_{12}^{\mathrm{real}}=64\pi\alpha_s N_C C_F\int[dp'dk]\left[\frac{m^2(Q^2+2m^2)}{(p^2-m^2)^2}+\frac{Q^2+2m^2-Q\cdot k}{p^2-m^2}-\frac{Q^4-4m^4}{2Q\cdot k(p^2-m^2)}+\frac{1}{2}\right.$$
$$\left.+\{(p^2-m^2)\to[(p'-k)^2-m^2]\}\right]\ , \tag{4.38}$$

with the phase-space integral given by

$$[dp'dk]=\int\frac{d^4p'd^4k}{(2\pi)^5}\tfrac{1}{2}\sin 2\phi_{p'}\tfrac{1}{2}\sin 2\phi_{p-k}\tfrac{1}{2}\sinh 2\theta_k\epsilon(p'_0)\epsilon(p_0-k_0)\delta(p'^2-m^2)\delta(k^2-\lambda^2)\delta((p-k)^2-m^2)\ , \tag{4.39}$$

using as integration variable $p'=p-Q$. Now we evaluate this integral for the photon at rest, $Q^\mu=(Q,0)$, by first writing the product of the three δ functions as

$$\frac{1}{4\omega E'}[\delta(k_0-\omega)+\delta(k_0+\omega)][\delta(p'_0-E')+\delta(p'_0+E')]\delta(Q^2+\lambda^2+2p'_0Q-2k_0Q-2p'_0k_0+2\sqrt{E'^2-m^2}\sqrt{\omega^2-\lambda^2}\cos\theta)\ , \tag{4.40}$$

with $E'=\sqrt{\mathbf{p}'^2+m^2}$, $\omega=\sqrt{\mathbf{k}^2+\lambda^2}$, and $|\cos\theta| \leq 1$.

Four different kinematical configurations, illustrated in Fig. 9, are acceptable.

(i) $p_0'=-E'$, $k_0=-\omega$, and $p_0-k_0=Q+\omega-E'>0$. It corresponds to gluon emission $q(E)\bar{q}(E') \rightarrow G(\omega)\gamma^*(Q)$, and the phase space [cf. Eq. (3.2) with $E_1=E'$] becomes

$$[dp'dk] \rightarrow -e^{\beta Q/2}P_{\text{em}} . \tag{4.41}$$

(ii) $p_0'=-E'$, $k_0=\omega$, and $p_0-k_0=Q-\omega-E'>0$. It corresponds to gluon absorption $q(E)\bar{q}(E')G(\omega) \rightarrow \gamma^*(Q)$, with the corresponding phase space [Eq. (3.5), $E_1=E'$]

$$[dp'dk] \rightarrow -e^{\beta Q/2}P_{\text{abs}} . \tag{4.42}$$

(iii) $p_0'=-E'$, $k_0=\omega$, but $p_0-k_0=Q-\omega-E'<0$. This is Compton scattering $\bar{q}(E')G(\omega) \rightarrow \bar{q}(E)\gamma^*(Q)$, with [cf. Eq. (3.6)]

$$[dp'dk] \rightarrow e^{\beta Q/2}P_{\text{Compton}} . \tag{4.43}$$

(iv) $p_0'=E'$, $k_0=\omega$, and $p_0-k_0=Q-\omega+E'>0$. This is also Compton scattering $q(E)G(\omega) \rightarrow q(E')\gamma^*(Q)$. Transforming $E' \rightarrow E=Q-\omega+E'$ it is the same as (iii).

From this together with Eq. (4.38) we find indeed that $\tilde{\Pi}_{12}^{\text{real}}$ contains all the real gluon processes in the same form as discussed in Sec. III A. Therefore the corresponding contribution to the dilepton rate is the same as R_{real}^{S} in Eq. (3.51), when the limit $m,\lambda \rightarrow 0$ is considered.

To summarize this section we find that the two-loop calculation of $\tilde{\Pi}_{12}$ leads to the same result as the alternative amplitude approach.

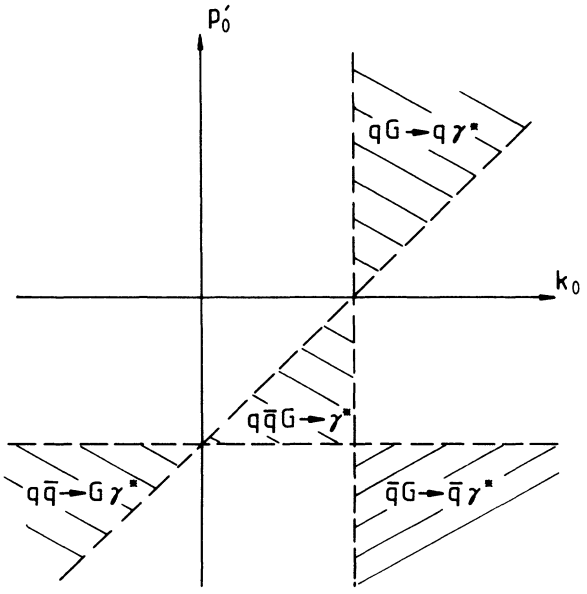

FIG. 9. Kinematically allowed regions in the (p_0',k_0) plane for the phase-space integral of Eq. (4.39). The boundaries are simplified by taking the limiting case of vanishing quark and gluon masses.

V. CONCLUSIONS

Using the framework of real-time perturbative QCD at finite temperature we have shown that the $O(\alpha_s)$ contribution to the lepton pair production rate is finite when the gluon and quark masses, used as regulators, are put to zero.

The thermo field formalism has proven to be quite efficient in this analysis of the production rate and of the related imaginary part of the thermal vacuum-polarization tensor. The last approach is reminiscent of the $T=0$ calculation for the total hadronic e^+e^- cross section. In this respect, one should emphasize that the $T=0$ limit of dilepton production in the plasma, is usefully related to the $T=0$ annihilation cross section and not to the hadronic Drell-Yan pair production process.

Actually as a result of this study we find that the dilepton rate up to $O(\alpha_s)$ may be written in the massless limit as

$$R \simeq \frac{1}{2\pi}N_C Q^2 n_F^2(Q/2)\left[1+\frac{3}{4}C_F\frac{\alpha_s}{\pi}+\frac{\alpha_s}{\pi}f(\beta Q)\right], \tag{5.1}$$

where the function f does not contain large logarithms and vanishes in the limit $\beta Q \rightarrow \infty$.

Although we have no insight yet on higher orders, we believe that the cancellations of IR and mass singularities at $O(\alpha_s)$, may hopefully be generalized. On the other hand, the perturbative calculation of the thermodynamic potential in finite-temperature non-Abelian gauge theories shows specific infrared problems.[29] These problems are linked in QCD to singularities of the gluon propagator at higher orders, not yet included in the present calculation. It is an open question whether this "plasmon" puzzle[14] shows up in the specific case of lepton pair production at finite temperature.

Leaving this question aside, the cancellation of divergences at $O(\alpha_s)$ is a positive feature. It gives a sounder basis to the phenomenological studies of lepton pair production as a signal for the formation of the quark-gluon plasma.

ACKNOWLEDGMENTS

Useful discussions with T. Altherr, P. Aurenche, T. Becherrawy, M. Fontannaz, and M. Le Bellac are gratefully appreciated. Partial support of this work by Projets de Cooperation et d'Echange (PROCOPE) is kindly acknowledged. The Centre de Physique Théorique is Laboratoire propre du CNRS. The Laboratoire de Physique Théorique et Hautes Énergies is Laboratoire associé du CNRS.

APPENDIX A: INTEGRALS

In this appendix we summarize the various integrals encountered in the main text. We systematically keep only IR and mass singular terms by considering the limit $m,\lambda \rightarrow 0$. The calculations are performed in the photon rest frame.

First we consider two integrals, independent of temperature, which appear in the calculation of real diagrams. We note that

$$I_1=\lim_{m\to 0}\lim_{\lambda\to 0}\int_\lambda^{Q/2}\frac{d\omega}{\omega}\left[I_1^S(\omega)-\ln\frac{1+v}{1-v}\right] \tag{A1}$$

is finite for $\lambda\to 0$, where $I_1^S(\omega)$ is given by Eq. (3.16) and $v=(1-4m^2/Q^2)^{1/2}$. Let us write I_1^S as

$$I_1^S(\omega)=\ln\left[\frac{(\omega+\kappa v)^2}{4\kappa^2+\lambda^2\frac{Q^2}{m^2}}\right]+\ln\frac{Q^2}{m^2}\ , \tag{A2}$$

where $\kappa=(\omega^2-\lambda^2)^{1/2}$. Then we obtain, in the limit $m,\lambda\to 0$,

$$\begin{aligned}I_1&\simeq\int_\lambda^{Q/2}\frac{d\omega}{\omega}\ln\left[\frac{(\omega+\kappa)^2}{4\kappa^2+\lambda^2\frac{Q^2}{m^2}}\right]\\&\simeq\int_1^\infty\frac{dx}{x}\ln\left[\frac{(x+\sqrt{x^2-1})^2}{4(x^2-1)+Q^2/m^2}\right]\\&\simeq-\frac{1}{4}\ln^2\frac{Q^2}{m^2}+\ln 2\ln\frac{Q^2}{m^2}\ ,\end{aligned} \tag{A3}$$

letting $\omega=\lambda x$. The last integral is derived in Ref. 22. In a similar way we treat

$$\begin{aligned}I_2&=\lim_{m\to 0}\lim_{\lambda\to 0}\int_\lambda^{Q/2}d\omega\, I_2^S(\omega)\\&\simeq\frac{vQ^2}{m^2}\left[\int_1^\infty dx\left[\frac{\sqrt{x^2-1}}{x^2-1+\frac{Q^2}{4m^2}}-\frac{1}{x}\right]+\ln\frac{Q}{\lambda}\right]\\&\simeq-\frac{vQ^2}{m^2}\ln\frac{\lambda}{m}\ ,\end{aligned} \tag{A4}$$

where $I_2^S(\omega)$ is given by Eq. (3.17).

Next we turn to temperature-dependent integrals, and define

$$I_S=\int_\lambda^{Q/2}\frac{d\omega}{\omega}n_B(\omega)I_1^S(\omega)\ , \tag{A5}$$

$$I_A=2\pi\frac{m^2}{vQ^2}\int_\lambda^{Q/2}d\omega\, n_B(\omega)I_2^S(\omega)\ , \tag{A6}$$

$$\begin{aligned}I_0&=\frac{2\pi}{vQ}\ln\frac{1+v}{1-v}\int_0^\infty\omega\, d\omega\, n_B(\omega)\\&\simeq\frac{2\pi}{Q}\ln\frac{Q^2}{m^2}I_B\ ,\end{aligned} \tag{A7}$$

with

$$I_B=\frac{\pi^2}{6}T^2\ , \tag{A8}$$

and, similarly,

$$\begin{aligned}J_0&=\frac{2\pi}{vQ}\ln\frac{1+v}{1-v}\int_m^\infty\sqrt{E^2-m^2}\,dE\, n_F(E)\\&\simeq\frac{2\pi}{Q}\ln\frac{Q^2}{m^2}I_F\ ,\end{aligned} \tag{A9}$$

with

$$I_F\simeq\frac{\pi^2}{12}T^2 \tag{A10}$$

in the massless limit. In the calculation of virtual diagrams one encounters [cf. Eq. (3.36)]

$$I=\int d^4k\, n_B(k)\delta(k^2-\lambda^2)\frac{1}{(2k\cdot p_1+\lambda^2)(2k\cdot p_2-\lambda^2)}=\tfrac{1}{4}\int d^3k\int\frac{dk_0}{2\omega}n_B(k)\frac{\delta(k_0+\omega)+\delta(k_0-\omega)}{(\omega E_p-\mathbf{k}\cdot\mathbf{p})(\omega E_p+\mathbf{k}\cdot\mathbf{p})}\ , \tag{A11}$$

which becomes, for $E_p=Q/2$ and $v=p/E_p$,

$$I=\frac{2\pi}{vQ^2}I_S\ . \tag{A12}$$

From Eq. (3.38) we find the principal-value integral for $m\to 0$:

$$I'=\mathrm{Re}\int d^4l\, n_F(l)\delta(l^2-m^2)\frac{1}{(p-l)^2(Q^2-2Q\cdot l+i\varepsilon)}\simeq\frac{\pi}{Q^2}\ln\frac{Q^2}{m^2}P\int\frac{l\,dl}{l^2-Q^2/4}n_F(l)\ . \tag{A13}$$

The integrals, which enter in the calculation of the self-energy diagrams after the expansion around $\not{p}=m$ [cf. Eq. (3.41)] is performed, are, in turn with $p^2=m^2$,

$$I_A=2m^2\int d^4k\, n_B(k)\delta(k^2-\lambda^2)\frac{1}{(2p\cdot k-\lambda^2)^2}\ , \tag{A14}$$

which when worked out are identical to Eq. (A6),

$$\begin{aligned}I^\mu&=\int d^4k\, n_B(k)\delta(k^2-\lambda^2)\frac{k^\mu}{2p\cdot k-\lambda^2}\\&=\int\frac{d^3k}{2\omega}n_B(\omega)\frac{(\omega,\mathbf{k})}{\omega E_p-\mathbf{k}\cdot\mathbf{p}}\ ,\end{aligned} \tag{A15}$$

with I_0 identical to Eq. (A7) and

$$L^{\mu}=-\frac{1}{E_p}\int d^4k\, n_B(k)\delta(k^2-\lambda^2)\frac{k_0k^{\mu}}{(2p\cdot k-\lambda^2)^2}$$
$$=-\frac{1}{4E_p}\int d^3k\, n_B(\omega)\frac{(\omega,\mathbf{k})}{(\omega E_p-\mathbf{k}\cdot\mathbf{p})^2}\ , \qquad \text{(A16)}$$

from which the relation in Eq. (3.43) follows. Further integrals evaluated on shell, $p^2=m^2$ [cf. Eq. (3.45)], are

$$J^{\mu}=\int d^4l\, n_F(l)\delta(l^2-m^2)\frac{l^{\mu}}{(p+l)^2}$$
$$=\int\frac{d^3l}{2E_l}n_F(l)\frac{(E_l,\mathbf{l})}{E_pE_l-\mathbf{p}\cdot\mathbf{l}+m^2}\ , \qquad \text{(A17)}$$

with $E_l=(l^2+m^2)^{1/2}$ and J_0 explicitly given in Eq. (A9),

$$K^{\mu}=-\frac{1}{E_p}\int d^4l\, n_F(l)\delta(l^2-m^2)\frac{(l_0+E_p)l^{\mu}}{(p+l)^4}\ . \qquad \text{(A18)}$$

Since

$$\int d^4l\, n_F(l)\delta(l^2-m^2)\frac{m^2(l_0+E_p)}{(p+l)^4} \qquad \text{(A19)}$$

is finite for $m\to 0$, Eq. (3.46) follows. Other integrals appearing in Secs. III and IV do not have IR and mass singular behavior, e.g.,

$$\int d^4k\, n_B(k)\delta(k^2-\lambda^2)=4\pi I_B\ , \qquad \text{(A20)}$$

$$\int d^4l\, n_F(l)\delta(l^2-m^2)=4\pi I_F\ , \qquad \text{(A21)}$$

and [cf. Eq. (3.45)]

$$J_A=2m\int d^4l\, n_F(l)\delta(l^2-m^2)\frac{1}{(p+l)^2}\ , \qquad \text{(A22)}$$

for $p^2\neq m^2$. Finally, we note that in the massless limit the singular integrals I_S and I_A have been incorrectly calculated in Ref. 6: e.g., I_S is not equal to $\ln|1+v/1-v|\int(d\omega/\omega)n_B(\omega)$ in the limit $m,\lambda\to 0$ as written in Ref. 6. In order to calculate these integrals one should use the same techniques as for the calculation of I_1 in Eqs. (A1)–(A3). Since, however, we are only interested in the cancellation of singular contributions, we do not need integrated expressions of I_S and I_A.

APPENDIX B: CANCELLATION OF δ^2 SINGULARITIES

Following Refs. 12 and 17 we show that the $[\delta(p^2-m^2)]^2$ singularities present in each of the four terms for $\delta S_{12}(p)$ in Eq. (4.18) cancel at $O(\alpha_s)$. A straightforward derivation starts by expressing the self-energy matrix Σ_{ab} in terms of the complex function Σ [cf. Eqs. (4.20)–(4.21)]:

$$\Sigma_{11}=-\Sigma_{22}^{*}=\cos^2\phi_p\Sigma+\sin^2\phi_p\Sigma^{*}\ , \qquad \text{(B1)}$$

$$\Sigma_{12}=-\Sigma_{21}=\epsilon(p_0)\sin\phi_p\cos\phi_p(\Sigma-\Sigma^{*})\ . \qquad \text{(B2)}$$

With the representation for $\tilde{S}_{ab}$ of Eq. (2.17) δS_{12} may be written as

$$i\delta S_{12}(p)=i\epsilon(p_0)\tfrac{1}{2}\sin 2\phi_p(\not p+m)\Sigma(p)(\not p+m)\{[2\pi\delta(p^2-m^2)]^2\sin^2\phi_p\cos^2\phi_p$$
$$+2\pi\delta(p^2-m^2)(\cos^2\phi_p i\tilde{S}_{11}-\sin^2\phi_p i\tilde{S}_{22})-\tilde{S}_{11}i\tilde{S}_{22}\}+\text{c.c.} \qquad \text{(B3)}$$

Since

$$i\tilde{S}_{11}=(i\tilde{S}_{22})^{*}=\tilde{S}-\sin^2\phi_p 2\pi\delta(p^2-m^2)\ , \qquad \text{(B4)}$$

the cancellation of the ill-defined δ^2 singularities is found. Taking into account that

$$\tilde{S}(p)+\tilde{S}^{*}(p)=2\pi\delta(p^2-m^2)\ , \qquad \text{(B5)}$$

the result given in Eq. (4.19) follows immediately. In principle, all these manipulations go through with the regularized form[16]

$$\delta(p^2-m^2)\to\frac{1}{\pi}\frac{\eta}{(p^2-m^2)+\eta^2}\ , \qquad \text{(B6)}$$

with the limit $\eta\to 0$ taken after the sum of the four terms for δS_{12} is performed.

[1]See, for a review and references, J. Cleymans, R. V. Gavai, and E. Suhonen, Phys. Rep. **130**, 217 (1986).

[2]See, for example, *Quark Matter '87*, proceedings of the Sixth International Conference on Ultra-Relativistic Nucleus-Nucleus Collisions, 1987, edited by H. Satz, H. J. Specht, and R. Stock [Z. Phys. C **38**, (1988)].

[3]E. L. Feinberg, Nuovo Cimento **34A**, 391 (1976); E. V. Shuryak, Yad. Fiz. **28**, 796 (1978) [Sov. J. Nucl. Phys. **28**, 408 (1978)]; Phys. Lett. **78B**, 150 (1978); Phys. Rep. **61**, 71 (1980); G. Domokos and J. I. Goldman, Phys. Rev. D **23**, 203 (1981); K. Kajantie and H. Miettinen, Z. Phys. C **9**, 341 (1981); **14**, 357 (1982); R. C. Hwa and K. Kajantie, Phys. Rev. D **32**, 1109 (1985); K. Kajantie, M. Kataja, L. McLerran, and P. V. Ruuskanen, *ibid.* **34**, 811 (1986).

[4]L. D. McLerran and T. Toimela, Phys. Rev. D **31**, 545 (1985).

[5]H. Umezawa, H. Matsumoto, and M. Tachiki, *Thermo Field*

Dynamics and Condensed States (North-Holland, Amsterdam, 1982); I. Ojima, Ann. Phys. (N.Y.) **137**, 1 (1981); H. Matsumoto, Y. Nakano, H. Umezawa, F. Mancini, and F. Marinaro, Prog. Theor. Phys. **70**, 599 (1983).

[6]J. F. Donoghue and B. R. Holstein, Phys. Rev. D **28**, 340 (1983); **29**, 3004(E) (1984); see also J. F. Donoghue, B. R. Holstein, and R. W. Robinett, Ann. Phys. (N.Y.) **164**, 233 (1985).

[7]T. Kinoshita, J. Math. Phys. **3**, 650 (1962); T. D. Lee and M. Nauenberg, Phys. Rev. **133**, B1549 (1964).

[8]H. D. Politzer, Nucl. Phys. **B129**, 301 (1977); D. Amati, R. Petronzio, and G. Veneziano, Nucl. Phys. **B146**, 29 (1978); S. B. Libby and G. Sterman, Phys. Rev. D **18**, 3252 (1978); A. H. Mueller, *ibid.* **18**, 3705 (1978); R. K. Ellis, H. Georgi, M. Machacek, H. D. Politzer, and G. G. Ross, Nucl. Phys. **B152**, 285 (1979); J. C. Collins, D. E. Soper, and G. Sterman, *ibid.* **B263**, 37 (1986).

[9]K. Kajantie and P. V. Ruuskanen, Phys. Lett. **121B**, 352 (1983).

[10]We previously presented a progress report of this study in Ref. 2, p. 265. The provisional conclusions that we had drawn, concerning remaining mass singularities, were based on an incomplete calculation where some contributions had been overlooked.

[11]H. A. Weldon, Phys. Rev. D **28**, 2007 (1983).

[12]R. L. Kobes and G. W. Semenoff, Nucl. Phys. **B260**, 714 (1985).

[13]R. L. Kobes and G. W. Semenoff, Nucl. Phys. **B272**, 329 (1986).

[14]See, for a review and references, N. P. Landsman and Ch.G. van Weert, Phys. Rep. **145**, 141 (1987).

[15]T. Matsubara, Prog. Theor. Phys. **14**, 351 (1955); R. P. Feynman, Phys. Rev. **91**, 1291 (1953); C. W. Bernard, Phys. Rev. D **9**, 3312 (1974); L. Dolan and R. Jackiw, *ibid.* **9**, 3320 (1974); S. Weinberg, *ibid.* **9**, 3357 (1974).

[16]A. J. Niemi and G. W. Semenoff, Nucl. Phys. **B230** [FS10], 181 (1984).

[17]H. Matsumoto, I. Ojima, and H. Umezawa, Ann. Phys. (N.Y.) **152**, 348 (1984).

[18]J. Cleymans and I. Dadić, Bielefeld Report No. BI-TP 87/13, 1987 (unpublished).

[19]J. D. Bjorken and S. D. Drell, *Relativistic Quantum Mechanics* (McGraw-Hill, New York, 1964).

[20]C. Itzykson and J.-B. Zuber, *Quantum Field Theory* (McGraw-Hill, New York, 1980).

[21]To be completely consistent with the stated approximation, we keep terms $\ln\lambda \ln(1+v)/(1-v)$ as such, since $\ln(1+v)/(1-v)=\ln Q^2/m^2+O(m^2)$.

[22]J. Kubar-André and F. E. Paige, Phys. Rev. D **19**, 221 (1979).

[23]With a different method this result is confirmed by an independent calculation using dimensional regularization for massless quarks by T. Altherr, P. Aurenche, and T. Becherrawy, Annecy Report No. LAPP-TH-221/88, 1988 (unpublished).

[24]The related process of deep-inelastic scattering at finite temperature has been studied in Ref. 18, and cancellation of IR and mass singularities is found.

[25]A related analysis in a scalar ϕ^3 field theory model in $D=6$ dimensions is given by T. Grandou, M. Le Bellac, and J.-L. Meunier, Nice Report No. NTH 88/9, 1988 (unpublished).

[26]T. Appelquist and H. Georgi, Phys. Rev. D **8**, 4000 (1973).

[27]A. Zee, Phys. Rev. D **8**, 4038 (1973).

[28]F. Ruiz Ruiz and R. F. Alvarez-Estrada, Z. Phys. C **34**, 131 (1987).

[29]A. D. Linde, Phys. Lett. **96B**, 289 (1980); D. J. Gross, R. D. Pisarski, and L. G. Yaffe, Rev. Mod. Phys. **53**, 43 (1981).